LISA Technology Status Summary

Stephen M. Merkowitz, Jeffrey C. Livas, Peiman G. Maghami, and James I. Thorpe
NASA Goddard Space Flight Center

Glenn DeVine, William M. Klipstein, Kirk McKenzie, Daniel A. Shaddock, Robert E. Spero, Brent Ware, and John K. Ziemer
NASA Jet Propulsion Laboratory

Luigi d'Arcio, David Nicolini, and Marcello Sallusti
European Space Research and Technology Center

Gerhard Heinzel
University of Hannover

Stefano Vitale
University of Trento

Reference	LISA-MSE-RP-0001
Issue	1
Revision	0
Date of issue	April 7, 2009

Executive Summary

All of LISA's core subsystems existed in some form at the beginning of the LISA technology development effort. **No new "inventions" were required, only an incremental performance increase and additional functionality from proven technology.** Nearly all the technologies that require development are those directly related to the science measurements; the spacecraft bus can be build with existing, flight proven, technologies. Table 1 summarizes the current status of all items whose technology readiness level (TRL) is 6 or below.

Dedicated LISA technology development had already begun when the first detailed technology plan was written and independently reviewed in 1999. The LISA Project Office, formed in 2001, implemented and built upon this plan. Major updates to the technology development plan were made in 2003 and 2005, that took into account advances in the technology, maturation of the baseline architecture, changes in partnership responsibilities, and funding levels. This document summarizes the current state of the LISA technology development program and the major tasks left to complete.

Substantial progress has been made over the past several years in advancing the LISA architecture and technologies. Both the Technology Readiness and Implementation Plan (TRIP) review in 2003 and the independent Technology assessment in late 2005 concluded that LISA's development program was making good progress and was on-track.

The selection of LISA Pathfinder as a dedicated mission to demonstrate several key LISA technologies provided a major boost to the development effort. In particular, this effort led to several successful engineering models of the gravitational reference sensor (GRS). The Pathfinder GRS is designed to meet all of the LISA requirements and is currently undergoing the flight build.

Likewise, micronewton thrusters have advanced considerably due to the Pathfinder activities. Three different thruster technologies demonstrated they are capable of meeting the LISA thrust and thrust noise requirements. The remaining development work for LISA is focused on demonstrating and extending their lifetime. The ST-7 flight thrusters are now fully verified and are awaiting delivery to ESA. LISA Pathfinder has also down-selected to the cesium slit FEEP, with the indium needle FEEP development continuing as a backup.

It was originally believed that some aspects of the LISA acquisition and drag-free control design were high risk and required technology development. However, control strategies and designs have matured over the course of the past few years to the point it is now demonstrated, using several independently developed high fidelity simulations, that standard control systems are capable of meeting the LISA requirements. Many of the drag-free algorithms will be fully validated on LISA Pathfinder providing further confidence in their performance.

LISA interferometry has also benefited from LISA Pathfinder. The Pathfinder optical bench uses the same construction techniques as the LISA bench and exceeds the LISA stability requirements. The Pathfinder flight qualified laser is suitable for use as the LISA seed laser. The LISA project has several activities ongoing to further improve these technologies.

The techniques for performing the phase measurement have also advanced considerably. Recent developments include methods for interpolating the data on ground that significantly simplify the flight system requirements. A breadboard phasemeter meeting LISA requirements was developed, and an implementation of locking the lasers to the length of the LISA arms that will dramatically

suppress the laser frequency noise was also developed. Laboratory demonstrations of these techniques have been very successful and are being upgraded with more realism and fidelity.

Technology	Current TRL	Rationale
Gravitational Reference Sensor	5-6	LISA Pathfinder GRS passed CDR. Low-frequency verification underway.
Optical Assembly Pointing Mechanism	6	Requirements for folded lever arm design can be met by mechanisms qualified for LISA Pathfinder.
Point Ahead Actuator	3	Similar mechanisms exist. Prototypes currently being verified.
Laser System	4-6	Laser components for LPF and TerraSAR-X missions are at TRL 6 but system level performance for LISA needs to be verified.
Laser Frequency Noise Suppression	4-5	Laser frequency noise and clock noise correction demonstrated on interferometry testbed.
Phase Measurement System	4-5	Documented in "LISA Phasemeter Technology Assessment and Report," LIMAS 2009-002.
Optical System	5-6	Optical system requires no new materials or techniques. The LISA optical bench uses the same process as the LISA Pathfinder bench, which has demonstrated better than LISA requirements.
Micronewton Thrusters	5-6	Three candidate thrusters exist that can all meet the LISA performance requirements: colloid micronewton thruster (CMNT) made by Busek Co. in Boston, indium needle field emission electric propulsion (FEEP) thruster made by ARC Seibersdorf in Austria, and cesium slit FEEP made by ALTA S.p.A. in Italy, which are all being developed in parallel to minimize risk for LISA. The CMNT and cesium slit FEEP will both be demonstrated on LISA Pathfinder. The CMNT flight hardware has completed all qualification, integration and test activities successfully. Cesium slit FEEP flight units are being fabricated.

Table 1: Current technology readiness level (TRL) off all LISA technologies under development.

1 Introduction

1.1 LISA Mission Overview

The Laser Interferometer Space Antenna (LISA) mission will be sensitive to gravitational waves from astrophysical sources such as black hole, white dwarf, and neutron star binaries. LISA is comprised of three identical spacecraft separated by 5 million kilometers nominally forming an equilateral triangle. Each spacecraft (S/C) encompasses two freely floating proof masses that are the references for the gravitational wave measurement. Each leg of the triangle acts as a single arm of an interferometer that is used to measure any change in the distance between the distant proof masses.

The three spacecraft are placed in heliocentric orbits 20° behind the Earth as shown in Figure 1. The orbits are chosen to keep the three baselines as close to equal as possible over the mission lifetime. The spacecraft at the corners house two proof masses and interferometry equipment.

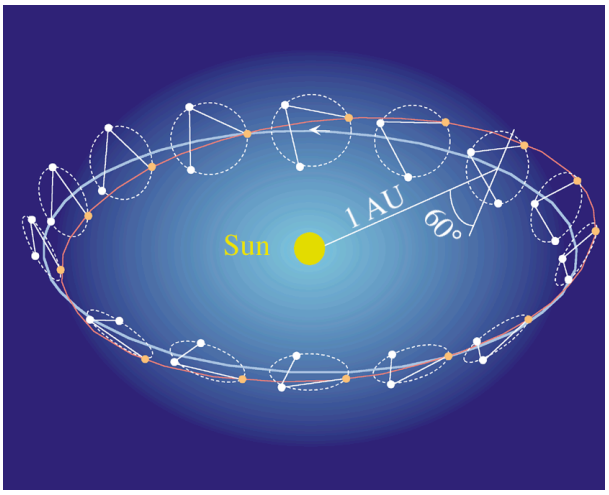

Figure 1: The LISA orbits do not require any regular adjustments to maintain the formation throughout the life of the mission. The spacecraft are represented by 3 dots in the snapshots of the formation's annual motion around the Sun. The inclined circle running through the same dot in each snapshot traces the orbit of one spacecraft.

The three spacecraft form a nearly equilateral triangle that appears to cartwheel around the Sun once per year. The measured baselines extend from a proof mass in one spacecraft to another proof mass in a distant spacecraft. Hence the proof masses are the measurement fiducials defining the endpoints of the monitored distance. The orbits of the three spacecraft are identical except for the phasing of their inclinations. The plane of the triangle is inclined 60° to the Earth's ecliptic plane. This geometry has the added benefit of a very benign environment, and a constant solar illumination angle on the spacecraft, thereby reducing unwanted disturbances.

The proof masses are protected from disturbances by careful design and "drag-free" operation. In drag-free operation, the mass is free-falling, but a housing around the proof mass senses the relative position of proof mass and spacecraft, and a control system commands the spacecraft's thrusters to follow the free-falling mass. This can be done with two proof masses, following each in only its sensitive direction. Drag-free operation keeps force gradients arising in the spacecraft from applying time-varying disturbances to the proof masses.

The distance between each spacecraft is monitored interferometrically using a series of one-way measurements. The optical phases of both beams at each vertex are measured separately, and the gravitational wave signal is contained in the data streams from these six one-way links. The minimum data suite for signal detection is four links, or two legs, corresponding to a Michelson interferometer. Slow orbital motion causes the leg lengths to differ by approximately 1%, which results in laser frequency noise contaminating the phase measurements. Without correction, laser frequency noise would be larger by eight orders of magnitude than the inherent picometer-scale

sensitivity of LISA. Unlike the gravitational wave signal, which appears as a differential change in leg length, laser frequency fluctuations are common to the Michelson legs. The four data streams can be time-shifted and combined to synthesize an equal-arm Michelson interferometer, which is insensitive to laser frequency noise but retains sensitivity to signal. This method of processing phase measurements is known as time-domain interferometry (TDI). The time-shifting requires a knowledge of the differential delay, or range, between phase measurements to ns-scale accuracy. Range measurement is implemented by injecting sideband modulation on the laser beams.

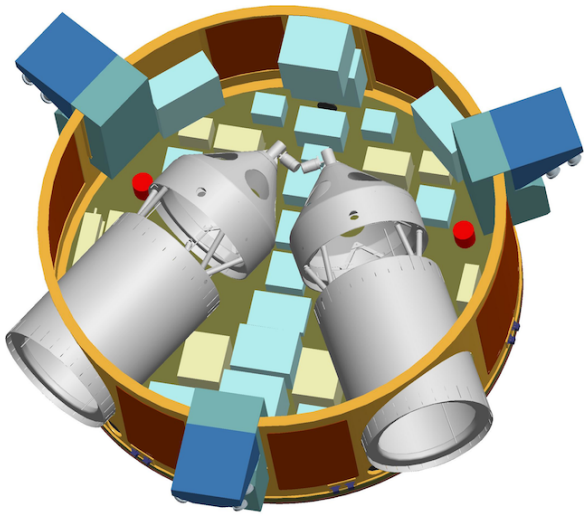

Figure 2: The LISA spacecraft is designed to provide a disturbance free environment for the scientific payload. The cutaway drawing shows the two payload tubes that provide a high level of thermal isolation to the optical assemblies.

The disturbance spectrum and the noise floor of the ranging system conspire to give a useful measurement bandwidth from $3x10^{-5}$ to 0.1 Hz. The three arms can simultaneously measure both polarizations of quadrupolar waves. The source direction from continuous sources is decoded from amplitude, frequency, and phase modulation caused by annual orbital motion.

The constellation of three coordinated spacecraft, each with its complement of scientific equipment, make up the LISA instrument. Since each spacecraft and its payload is an integrated part of the scientific instrument, the spacecraft/payload combination is referred to as a "sciencecraft." The three LISA sciencecraft are essentially identical. A recent mechanical layout is shown in Figure 2.

The demands of gravitational wave detection naturally organize the equipment of each sciencecraft around two considerations: interferometric displacement measurement and disturbance reduction. The important functional constituents of the Interferometry Measurement System (IMS) are a pre-stabilized laser subsystem, interferometry optics, a phase measurement system and a post-processed laser and clock frequency noise correction scheme. The Disturbance Reduction System (DRS) comprises the proof masses, their enclosures with sensing and actuation hardware and discharge subsystems, the control systems that implements drag-free operation, thrusters capable of continuous micronewton level thrust, and a host of other spacecraft and payload design features to reduce disturbances.

The IMS is a continuous ranging system, like spacecraft tracking, except it uses optical frequencies and is capable of resolving approximately a millionth of an optical wavelength. The ranging system senses inter-spacecraft Doppler motions, temporal variations of laser frequency, temporal variations of the optical pathlength between proof masses and temporal variations in the ultra-stable oscillator used to sample the data. A phasemeter measures frequency variations in the beat signal between a returning beam and the local laser and between the two local lasers serving the two optical benches. The science signal appears as a millihertz phase modulation on a megahertz beat signal. The important constituents of the IMS are:

- Transmit/receive telescope,
- Optical bench with interferometry optics and laser stabilization,
- 1.064μm Nd:YAG non-planar ring oscillator master laser, electro-optic phase modulator, 1 W fiber amplifier, plus spare,
- Phasemeter electronics, including ultra-stable oscillator,
- Fiber link for comparing laser phase between two arms.

The Disturbance Reduction System (DRS) is a collection of design choices and specific hardware to keep unwanted forces from moving the proof masses in a manner that would be confused with a gravitational wave. The choice of orbits places the spacecraft in a very benign environment where the most significant disturbance is the variation in the solar constant. Thermal, magnetic and self-gravity disturbances are controlled by careful design. Drag-free operation plays an important role in reducing local disturbances. Electrostatic charging of the proof mass by cosmic rays is actively controlled by UV lamps. More than 35 physical effects are taken into consideration in order to hold the residual acceleration of the proof masses down to $3\text{x}10^{-15}$ m/s^2/√Hz at 0.1 mHz and above.

The specific subsystems for disturbance reduction are:

- The Gravitational Reference Sensor (GRS),
- Micronewton thrusters,
- Optical assembly articulation mechanism
- Drag-free and attitude control system.

There are two GRSs per sciencecraft, corresponding the ends of the two baselines. The GRS consists of the proof mass, its reference housing and the charge control subsystem. The proof mass is a 46 mm, gold-coated cube made of a gold-platinum alloy with very low magnetic susceptibility. The reference housing has electrodes for electrostatically sensing the proof mass position, and for applying very small forces in directions orthogonal to the measurement axis. There is no mechanical contact between the proof mass and its surroundings with gaps that range between 3 and 4 mm. The main optical system is also used to measure the proof mass position relative to the optical bench more precisely, thereby improving drag-free performance.

1.2 Scope

The purpose of this document is to provide a summary of the current status of the LISA technology. It provides the current "snapshot" of the technology development planning and implementation. A more indepth discussion of the technology status can be found in the "LISA Technology Status Report" [1]. A detailed discussion of the LISA technology development plan can be found in reference [2].

1.3 Technology Assessment

The purpose of the LISA technology development effort is to reduce project risk by addressing particularly high risk/high impact items before investing in detailed designs. It includes both component and subsystems where research and development is required to mature the technology. Some components and subsystems need not be addressed through the technology development program, as they are sufficiently mature that their development and validation is within the scope of the flight systems offices. The goal of the technology development program is to raise high-risk

components and minor subsystems to Technology Readiness Level (TRL) 6 by Preliminary Design Review (PDR).

Shown in Figure 3 is the top level LISA Product Breakdown Structure highlighting the high-risk items that have been included in the LISA technology development effort. Highlighted in yellow are areas that require research and development to improve the performance of existing systems. For these areas a clear progression of technology readiness levels is part of the development plan. Highlighted in cyan are areas where system level laboratory demonstrations are underway to lower risk and solve engineering challenges, but no formal technology development is required. Finally, highlighted in blue are areas where the technology risk has been retired and the performance has been demonstrated to meet the LISA requirements. A more detailed assessment of the TRL for all major subsystems is shown in Table 2 and Table 3 below.

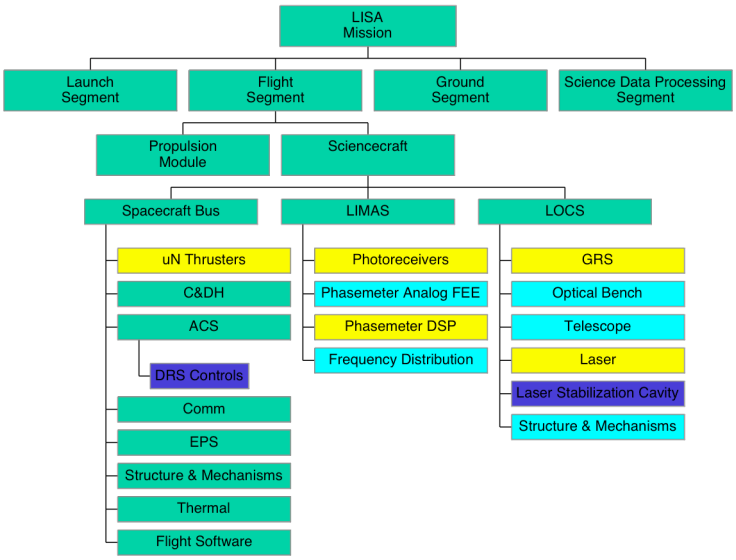

Figure 3: This Product Breakdown Structure of the LISA mission highlights in yellow areas that contain technology development. Highlighted in cyan are areas where system level laboratory demonstrations are underway to lower risk and solve engineering challenges, but no formal technology development is required. Finally, highlighted in blue are areas where the technology risk has been retired.

Technology	TRL	Rationale
Gravitational Reference Sensor	5-6	LISA Pathfinder GRS passed CDR. Low-frequency verification underway.
Optical Assembly Pointing Mechanism	6	Requirements for folded lever arm design can be met by mechanisms qualified for LISA Pathfinder.
Point Ahead Actuator	3	Similar mechanisms exist. Prototypes currently being verified.
Laser System	4-6	Laser components for LPF and TerraSAR-X missions are at TRL 6 but system level performance for LISA needs to be verified.
Laser Frequency Noise Suppression	4-5	Laser frequency noise and clock noise correction demonstrated on interferometry testbed.
Phase Measurement System	4-5	Documented in "LISA Phasemeter Technology Assessment and Report," LIMAS 2009-002.
Optical System	5-6	Optical system requires no new materials or techniques. The LISA optical bench uses the same process as the LISA Pathfinder bench, which has demonstrated better than LISA requirements.

Table 2: Current TRL assessment for all major technologies within the scientific compliment. For a more complete description of all the payload subsystems see reference [3].

S/C Subsystem	S/C Item	TRL	Description/Rationale
Attitude control system (ACS)			The ACS maintains pointing during the Cruise and Safe modes and other modes leading to the Science mode. The majority of the ACS has modest requirements; the more stringent pointing requirements are the responsibility of the Disturbance Reduction System (DRS) controls, which constitutes the LISA Science mode. No new hardware technologies are required. Detailed simulations (i.e. SIMULINK) were performed and preliminary control laws were designed for both science and LISA acquisition modes.
	DRS Control Laws	>6	Responsible for the precision S/C attitude and position control during acquisition and science modes. Several high fidelity simulations have shown that standard control laws with proven flight heritage may be used. TRL assignment is based on the 2006 independent technology assessment.
	Star trackers	9	Multiple heritage systems available such as the μASC from DTU or the Ball CT602 will meet LISA requirements. The Star trackers are used during all ACS modes except Science, which demands a much more accurate cadre of sensors.
	Sun Sensors	9	Both Digital Sun sensors (DSS) and Coarse Sun sensors (CSS) can be used to safe the spacecraft, and in the case of DSS, to provide fine pointing during non-science normal operations. Multiple heritage DSS systems are available including those from Adcole, TNO/TPD, Galileo Avionica. CSS units from Adclode and EADS/Astrium have been extensively used in a variety of missions.
	Solid state gyros	9	Solid state gyros with no moving parts are preferred for their reliability and minimum disturbances to the payload. Available heritage systems include the Fibre Optic Gyros of EADS Astrium, ASTRIX200, which has flight heritage on PLEIADES HR, the Ring Laser Gyro developed by Honeywell through the Miniature Inertial Measurement Unit (MIMU) and the Quartz Oscillator Gyro (SSIRU) provided by Nothrop Grumman. The former comprises three orthogonal gyrometers (as well as three accelerometers) and is onboard Rosetta, Mars Express and Venus Express, and the latter is on-board Cassini. The leading candidate at this time is the Northrop Gruman FOG200, which is a Fiber Optic gyro.
Command and data handling			The command and data handling architecture employs a central processor unit within the On-board Computer (OBC) driving a standard serial bus (MIL STD 1553 and a router-based SpaceWire network) as the primary digital interface between the major elements of the S/C avionics. Several flight proven central processors are available including: BAE RAD750, RAD6000 SBC, and the RH-CF5208 (coldfire). All mathematical algorithms and models of the flight software run on the OBC, with the payload instruments serving at the level of sensors and actuators managed by dedicated cold redundant instrument controllers based on the rather simple microcontrollers (such as a 80C32) that cannot run complex control software but serve to manage the electrical interface down to the physical layer. No new technologies are required.
Communications			The telecommunication subsystem meets the modest 90 kbps downlink / 2 kbps uplink per spacecraft requirements with a radio frequency package comprised of two 30 cm high gain antennas, six low gain antennas, a Ka-band transponder, and associated electronics. A single mechanism is used to rotate the antenna in azimuth to provide Earth-tracking – the variation in Earth elevation is captured within the full width at half maximum of the antenna. No new technologies are required.
	High gain antennas & gimbals	9	Multiple heritage systems available such as those used on MRO, Cassini, and DS1.
	Traveling Wave Tube Amplifier (TWTA)	9	Multiple heritage systems available such as those used on MRO, Cassini, and DS1.

S/C Subsystem	S/C Item	TRL	Description/Rationale
Electrical Power			The power system comprises a Power Control & Distribution Unit (PCDU), solar array, and battery. The power system requirements are met by a conventional design with a 783 W EOL GaAs solar array and a 1.04 KWhr Li-Ion battery. The battery is only needed during the separation phase prior to pointing the solar array at the sun. The bus regulator is a Maximum Power Point Tracking (MPPT) design. No new technologies are required.
	Battery	9	Multiple heritage Li-Ion batteries are available.
	Solar array	9	Standard body mounted triple junction GaAs. Solar array is backwired to reduce stray magnetic fields.
Propulsion			The S/C propulsion system consists of micronewton thrusters and their associated electronics and propellant delivery system. New technology is required.
	Micronewton Thrusters	5-6	Three candidate thrusters exist that can all meet the LISA performance requirements: colloid micronewton thruster (CMNT) made by Busek Co. in Boston, indium needle field emission electric propulsion (FEEP) thruster made by ARC Seibersdorf in Austria, and cesium slit FEEP made by ALTA S.p.A. in Italy, which are all being developed in parallel to minimize risk for LISA. The CMNT and cesium slit FEEP will both be demonstrated on LISA Pathfinder. The CMNT flight hardware has completed all qualification, integration and test activities successfully. Cesium slit FEEP flight units are being fabricated.
Structures/Mechanisms			The S/C structure will be a unique, yet straightforward design that uses standard construction techniques and materials (mostly aluminum honeycomb composite). No new technologies are required. Detailed mechanical design and analysis has been performed.
	Separation System	9	Multiple heritage systems available such as the Lightband or SAAB CBOD.
Thermal			No non-standard technologies. Passive design. No new technologies are required. Detailed thermal design and analysis has been performed.
Harness			Standard flight harness can be used, but harness layout will be more precisely controlled than for a typical mission due to self-gravity requirements. No new technologies are required.

Table 3: Current assessment of all the major spacecraft bus subsystems. ***The micronewton thrusters are the only spacecraft item that requires technology development.*** For a detailed description of the spacecraft see reference [4].

1.4 Technology Management Approach

The roles and responsibilities of NASA and ESA are defined by the NASA-ESA Letter of Agreement [5] and the "LISA Project Agreement," [6]. The Project Agreement describes the tentative allocation of mission elements and the assignment of roles and responsibilities. This allocation assumes a specific flight system architecture, defined down to the subsystem and even the component level in special instances. Responsibility for flight-related products were tentatively assigned on the basis of technical expertise at the time of the agreement. These assignments will be revisited around the time of mission PDR, when technical capabilities, mission architecture and partner resources are better understood. However, these assignments are the basis of the current allocation of technology development responsibilities.

The LISA technology development plans were developed using the following approach:

1. The science requirements were flowed down to the subsystems to identify the driving requirements.
2. The present status of the technology supporting the baseline and alternative architectures was assessed.

3. The major risks to the baseline architecture were identified including the risk of meeting a critical requirement. Risk mitigations were developed that included the development of improved technologies.
4. The appropriate subsystem requirements were assigned to a technology item if there was a risk identified in meeting the requirement without additional technology development.
5. Key milestones and gates were defined for each technology to track the development progress.
6. Baseline schedules and budgets were developed for each technology item that took into account system engineering trade studies and other project activities that influence technical decisions and the implementation of off-ramps.

Within NASA, the flight element leads are responsible for the technology development activities in their area. However, the budget and schedule of the technology development is tracked separately to ensure it takes priority over normal formulation activities.

ESA supports a substantial amount of technology development through the Technology Readiness Programme (TRP) and the Core Technology Programme (CTP).. This support has funded major efforts on the Gravitational Reference Sensor at the University of Trento and interferometry work at AEI Hannover, as well as research programs at Imperial College and University of Glasgow. Further, the LISA Technology Package (LTP) on the LISA Pathfinder mission is a major part of ESA's technology development and an integral part of the main LISA mission. Consequently, LTP has been tightly focused on demonstrating LISA technology wherever possible. This approach leveraged the TRP support to prepare for LTP, and then the LTP effort to prepare for LISA very effectively. ESA is currently supporting additional LISA technology development contracts based on recommendations from the current formulation study.

The governments of ESA's member states are also important sources of financial support for technology development. Both the national space agencies and other science funding organizations (e.g., INFN in Italy) have and will continue to contribute very significant support to LISA technology development. For the purposes of Project planning, these contributions will be coordinated through ESA, and need not be considered further here. Hereinafter, any reference to the ESA role in technology development includes the participation of the European member states.

The ESA and NASA technology development efforts are aligned through common top-level planning. These plans are regularly assessed at the joint NASA/ESA Technical Interchange Meetings along with management meetings. During these meetings the status of the technology development is assessed along with the results of the system engineering trade studies. Modifications to the subsystem requirements are discussed at these regular meetings that take into account the maturation of the baseline architecture and the status of the technology development. Off-ramp decisions are also made at these joint meetings.

A critical part of the technology development plan are technology gates and their intermediate progress milestones. The gates are performance-based metrics traceable to the mission requirements. Failure to meet the gates will result in slippage of the Project schedule; the Project will not proceed past Preliminary Design Review until all of the technology gates are passed. The intermediate milestones serve to measure progress towards the gates.

In the past, the ESA and NASA portions of the LISA Project were to carry out parallel technology development, as a general risk mitigation strategy. However, due to budget constraints and an improving understanding of technology development needs, the Project decided to adopt a complementary approach to lower risk technologies, and dual development only where the risk is deemed sufficiently high. When the risk is high, both agencies will develop appropriate technologies

in a coordinated fashion. When the risk is lower, only the agency responsible for the associated flight deliverable will develop that technology.

1.5 LISA Pathfinder

LISA Pathfinder (LPF) is an ESA mission whose main scientific goal is to retire as much risk as possible from LISA technology and procedures that cannot be fully tested on the ground. LPF will carry two instrument packages: ESA's LISA Technology Package (LTP) and NASA's Space Technology 7 (ST7). The LISA related technologies contained in these packages are:

The Gravitational Reference Sensor (GRS),
Micronewton thrusters,
Disturbance Reduction System control laws,
Proof mass metrology laser interferometer.

The LTP consists of all of these items, while the ST7 package contains the thrusters and control laws; ST7 will use the LTP sensors for its demonstration.

Figure 4: The LISA Pathfinder spacecraft is currently undergoing integration and test in the Large European Acoustic Facility (LEAF) at ESTEC.

Four kinds of benefits accrue to LISA from a flight demonstration: First and most importantly, the demonstration flight will test a high fidelity system in a realistic environment. The conditions in LPF are very similar to those of LISA. Consequently, the performance objectives approach, but do not equal, those required for LISA. Second, the flight demonstration can validate the performance models with which to extrapolate the performance of the LISA instrumentation to the levels required by LISA. Third, the flight demonstration project gets the complete experience of building and verifying flight hardware; the vast majority of technical issues must be confronted. Finally, and importantly in the case of LTP, there is a substantial ground-test program associated with the demonstration flight that bears on LISA technology and LISA ground-based technology development in particular.

LPF will demonstrate several aspects of the technology at the system level to achieve these benefits:

- Gravitational free fall of a proof mass along the sensitive axis with a residual acceleration noise less than $3\times10^{-14}(1+(f/3\text{mHz})^2)$ m/s^2/$\sqrt{\text{Hz}}$ in a frequency band of $1\text{mHz} \le f \le 30\text{mHz}$.
- Relative proof mass-spacecraft position control to 1.8 nm/$\sqrt{\text{Hz}}$ in a frequency band of $1\text{mHz} \le f \le 30\text{mHz}$.
- Micronewton thruster thrust noise to 0.1 μN/$\sqrt{\text{Hz}}$ in a frequency band of $1\text{mHz} \le f \le 30\text{mHz}$.
- Relative proof mass-optical bench position sensitivity to 9.1×10^{-12} $(1+(f/3\text{mHz})^{-4})^{1/2}$ m/$\sqrt{\text{Hz}}$ in a frequency band of $1\text{mHz} \le f \le 30\text{mHz}$.

The performance levels required for LPF were chosen to be at a level that sufficiently reduces the risk to LISA while minimizing the cost for the demonstration mission. While **all the technologies are designed to meet LISA performance requirements**, Pathfinder cost constraints limit the spacecraft environment, operations, and the extent of ground-testing. The acceleration noise

requirement was relaxed to be about a factor of 7 worse than LISA due to the noisier spacecraft environment. The frequency requirement for all measurements was relaxed by a factor of 10 from the LISA requirement as a result of the accelerated test program and a modest mission life (~3 months). Risk reduction for LISA is maintained with these compromises as this level of performance will still meet LISA's minimum mission requirements.

Targeted experiments on Pathfinder will validate the LISA disturbance noise models. By exaggerating a number of disturbance sources (such as magnetic and thermal gradients) the Pathfinder experiments will be able to probe below the required noise floor to reduce the risk that any of these disturbances are larger than expected. Several spacecraft level techniques will also be validated on LPF that reduce the risk to LISA, such as:

- The management of time-dependent S/C thermoelastic distortion at low frequencies,
- The management of the S/C gravitational field and field gradient.

Details on the Pathfinder mission can be found in reference [7].

2 IMS Technologies

LISA observes gravitational waves by interferometrically monitoring the relative distance between the six freely falling proof masses aboard the three LISA S/C as shown in Figure 5. The elements used for this purpose are grouped together into what is called the Interferometry Measurement System (IMS). These components consist of a laser subsystem, a frequency stabilization subsystem, a phase measurement systems, an optical bench, and a telescope. The optical bench and telescope are mounted together as a single optical assembly that is fiber coupled to the laser subsystems. There are two optical assemblies per spacecraft and four laser subsystems arranged as two redundant pairs.

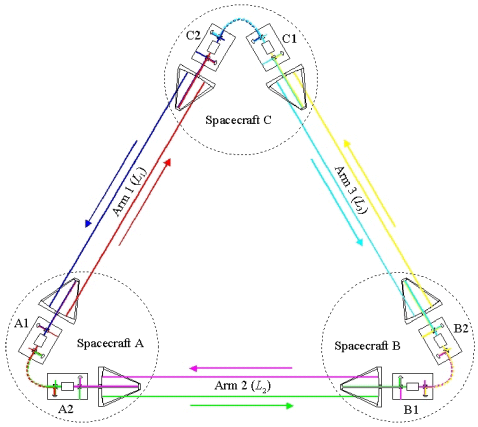

Figure 5: Distance variations between the three LISA spacecraft are measured with the Interferometry Measurement System (IMS).

The top level IMS requirement is to measure variations in the distance between pairs of proof masses with a sensitivity of at least

$$\sqrt{S_x} = 18\sqrt{1+\left(\frac{2\text{mHz}}{f}\right)^4}\ \text{pm}/\sqrt{\text{Hz}}\,,\ 0.03\ \text{mHz} \le \text{f} \le 0.1\text{Hz}$$

equivalent motion per mass. Approximately half of this design sensitivity is budgeted to shot noise on the main photodetectors.

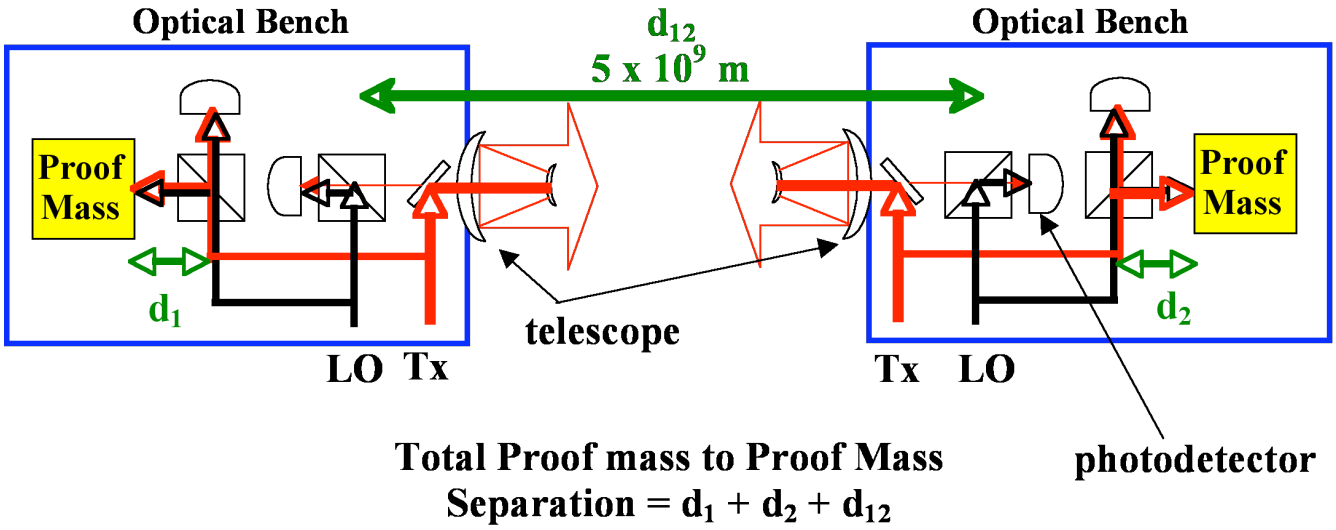

Figure 6: The IMS divides the measurement of the distance between proof masses into 3 parts: two parts are "short arm" interferometers and measure the movement of the proof mass with respect to the optical benches. The "long arm" is the separation between optical benches [11].

The distance measurement is divided conceptually into three parts as shown in Figure 6. Two of the parts represent the position of the proof masses with respect to their optical benches. These

two distances are of order 0.5 m and form the "short arm" part of the measurement. The distance between optical benches in different spacecraft, referred to as the "long arm" interferometer, is approximately 5 x 10^9 meters. Note that each measurement is made by a separate localized interferometer whose output is digitized by a phasemeter and recorded for processing. One advantage of separating the measurement into a short arm and long arm is that the short arm measurement is contained entirely within a single sciencecraft and so may be tested independently of the long arm measurement.

The majority of the IMS can be fully tested on the ground. The exception is the long-arm interferometer. The Pathfinder mission will be flying an optical bench with many of the design features as the LISA bench, providing an opportunity to test construction techniques and test procedures in a flight environment. The optical bench is discussed in more detail in Section 2.1.

2.1 Optical System

The LISA optical system consists of the optical bench, telescope, and the associated structures needed to support them. **No new technology is needed for the optical system**, although careful design and engineering is necessary to meet the requirements. The optical system can be fully verified on-ground and many of the same construction and test techniques are being used on LISA Pathfinder and have already exceeded several key LISA requirements.

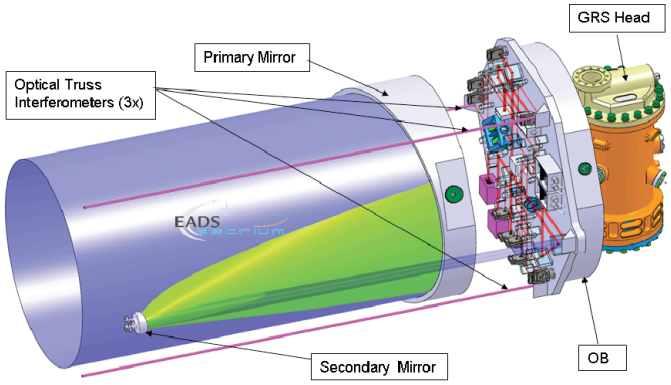

Figure 7: No new technology is required for the LISA optical system.

A telescope is required to send and receive the laser beams to and from the distant spacecraft. The baseline LISA telescope is a 40 cm diameter, off-axis design. Table 4 summarizes the high level performance requirements.

Parameter	Requirement	CBE	Units	Comments
Telescope wavefront error	λ/30	λ/40	waves	SILEX telescope
Telescope CTE	10^{-6}	2 x 10^{-8}	/°K	Zerodur, Schott [8]

Table 4: Summary of high level requirements for the telescope.

The required wavefront error of λ/30 is well within the capability of previously flown telescopes on missions such as SILEX and LORRI, The stability of the primary to secondary mirror spacing is of critical importance as this path length directly enters into the science measurement. Choosing materials with a low coefficient of thermal expansion (CTE) and placing them in a thermally quiet environment can achieve the required dimensional stability. For example, CTE's of 10^{-7} can be achieved with ULE glass near room temperature [9]. Modeling indicates that fluctuations of ~1 μK/√Hz is possible in a LISA-like orbit [10]. The net result is a dimensional stability on the order of 0.1 pm/√Hz.

Given the demonstrations and flight performance of similar telescopes, the LISA telescope is considered to be at TRL 5. The full telescope development effort is currently ongoing as part of the regular LISA formulation activities.

The optical bench is mounted behind the telescope assembly and contains the optics necessary to send and receive light to/from the telescope. It also hosts three distinct interferometers: one to combine the transmitted and received beams for the main science measurement (long arm), one to measure the motion of the proof mass relative to the bench (short arm), and one to lock the transmit lasers on the spacecraft together. It also contains the optics necessary to amplitude and frequency stabilize the lasers.

The LISA Optical Bench utilizes all the essential design, construction, and verification techniques already validated on the LISA Pathfinder optical bench. The Pathfinder OB engineering model successfully passed extensive performance and environmental testing, including vibration and thermal-vacuum and flight hardware will be delivered in July 2009. **Its demonstrated performance exceeds the LISA optical performance requirements by almost an order of magnitude.**

Figure 8 shows the results of tests of the LISA Pathfinder optical bench engineering model, showing that the measured performance of the entire subsystem is just slightly above 1 pm/√Hz with a requirement of 10 pm/√Hz.

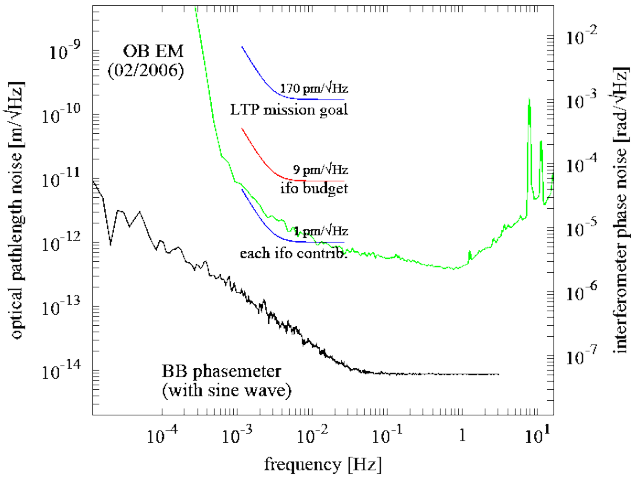

Figure 8: Test results of the LISA Pathfinder optical bench engineering model showing measured optical pathlength performance (green). The required performance for LISA is shown approximately by the red line at 9 pm/√Hz.

With the tools and techniques for building the LISA optical bench fully validated, the LISA formulation work is focused on the detailed design of the optical layout. This activity is ongoing as part of the regular LISA formulation activities. For example, ESA is currently starting the development of an Elegant Breadboard of the LISA Optical Bench. The main goal of the activity is the validation of key aspects specific to the LISA OB implementation including the use of polarizing interferometry for the science interferometer, the phase fidelity of the backside fiber connecting the two OBs on each spacecraft, the fiber switching devices for the redundant lasers, the on-bench acquisition sensors, and the optics for the interferometer pupil imaging.

2.2 Laser System

The laser system provides light to the LISA optical bench in order to i) send the light to the remote spacecraft for the main LISA science measurement, ii) act as the local oscillator beam for beating against the incoming light in the science interferometer, iii) provide the optical readout beam for the local measurements of the proof mass, and iv) provide a pair of optical sidetones whose phase accurately represents the local clock for transmission to the distant spacecraft. The laser system also provides modulation sidebands that can be used for information transfer (communications) and precision ranging between the spacecraft. The laser system currently baselined for LISA consists of a low power master laser followed by a fiber-coupled electro-optic phase modulator (EOM) and then a fiber amplifier (MOFA architecture) [17].

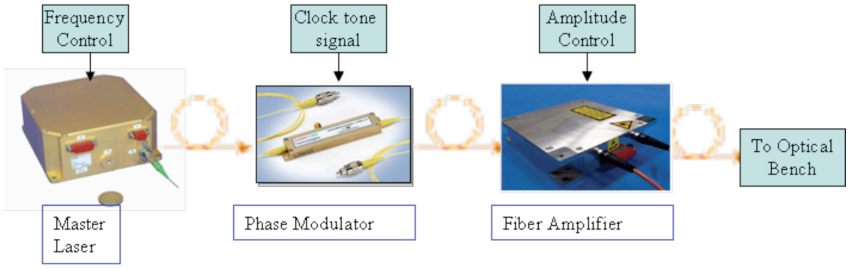

Figure 9 Elements of the LISA Laser System include a master laser, an electro-optic phase modulator, and a fiber amplifier.

The baseline master oscillator is a non-planar ring oscillator (NPRO), emitting 25mW at a wavelength of 1064nm, with a 50 kHz bandwidth actuator for frequency stabilization. Tesat GmbH (Germany) has developed and fully qualified a NPRO master laser which is flying since June 2007 on the TerraSAR-X and N-Fire missions and will fly on LISA Pathfinder mission in 2010. **This space qualified master laser has demonstrated all of the LISA performance requirements [18].**

An EOM is used to modulate clock noise onto the laser beam transmitted between spacecraft. A fiber-coupled EOM is baselined to minimize RF power requirements. A commercial fiber-coupled modulator running at 8 GHz **demonstrated better than required RF-to-optical phase stability** in laboratory tests [19], see Figure 10.

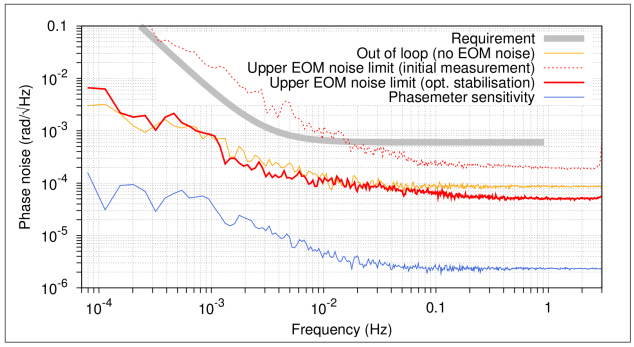

Figure 10: EOM RF-to-optical phase stability results.

A fiber amplifier is used to boost the laser power up to the required level. The Tesat space qualified fiber amplifier currently flying on TerraSAR-X has been operated at output powers of 1.2 W, to be compared to a LISA requirement of 2W optical power delivered to the Optical Bench. Characterization of a new fiber amplifier from TESAT, rated for output powers up to 5 W, is planned to start at AEI in March 2009.

Lifetime and non-statistical infant mortality are risks for the laser. Laser lifetime is likely to be dominated by the lifetime of the pump diodes. Tesat has developed a screening process to select single emitters with mean time to failure exceeding LISA requirements. Nevertheless, LISA will have redundant pump diode modules to mitigate the risk of pump diode failure. The LISA Pathfinder and TerraSAR-X lasers have enough redundancy in the pump diodes to guarantee a five year lifetime. In addition, LISA has redundant laser systems; and extensive burn-in of the flight units will be used to screen against early failures.

With the availability of space qualified laser components meeting LISA requirements, the major remaining task for LISA is to demonstrate the required performance at the system level. The main and long-standing issue is to demonstrate that the amplifier output is phase-stable with respect to the input laser phase and the modulation sidetones used for clock noise correction. In the fall of 2008, AEI Hannover succeeded in characterizing the differential phase noise of both a core-pumped and a cladding-pumped 1 W fiber amplifiers to the required sensitivity [18]. **Both devices fulfill the LISA differential phase noise requirement**, see Figure 11. The same investigation is planned for the Tesat 5 W amplifier.

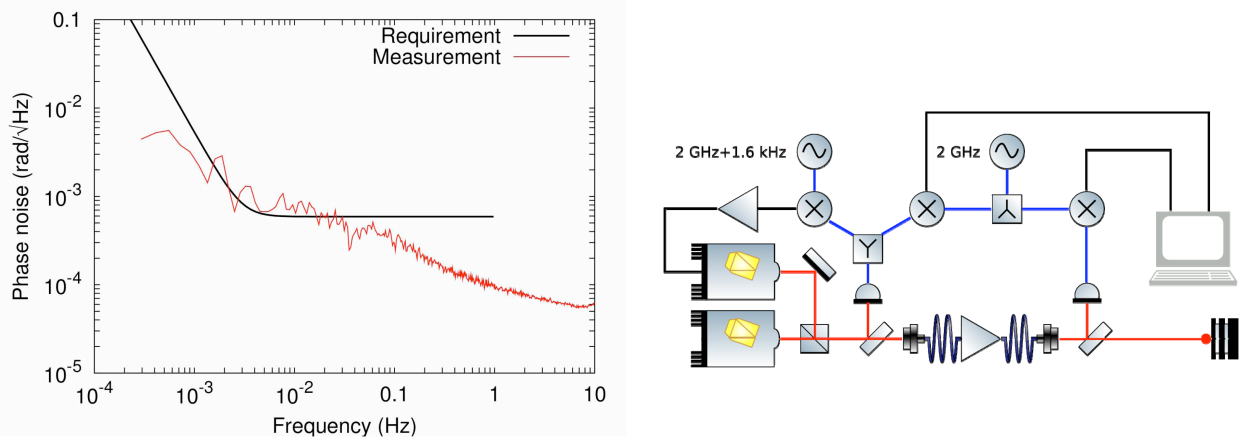

Figure 11: Left: differential phase stability results for a cladding-pumped amplifier operating at 1 W. The shown phase noise refers to the excess noise introduced by the fiber amplifier. Seed noise is not represented here. Right: measurement setup.

Capitalizing on these results, in Q2 2009 ESA will start a technology activity for the development of an Engineering Model of the full Laser Assembly for LISA, including master oscillator, EOM, fiber power amplifier, an opto-mechanical switch for acquisition purposes, and associated electronics. Main aspects to be demonstrated during this activity are:

- the space qualifiability of all laser optics and opto-electronic components. In particular, radiation hardness issues will be intensively studied in selection of space qualified fibers and electro-optical components.
- Performance demonstration of the Laser Assembly system, including the EOM and fiber amplifier phase stability requirements as described above
- lifetime performance
- environmental qualification of the Laser Assembly, including radiation hardness, vibration, and thermal cycling.

The Laser Assembly activity also includes the development of an EM of a tunable frequency reference for frequency pre-stabilization of the LISA laser. The frequency reference will be tunable in order to ensure compatibility with the LISA implementation of arm-locking.

Milestone	Date
Demonstrate seed laser at TRL6	*Completed*
Demonstrate EOM RF-optical-RF phase stability	*Completed*
Demonstrate low differential phase noise of fibre amplifier	*Completed*
Characterize 5W TESAT fiber amplifier	March 2009
Design complete EM Laser Assembly (ESA)	Q2 2010
Demonstrate complete Laser Assembly at TRL6 (ESA)	Q3 2011
Demonstrate tunable freq. reference at TRL5 (ESA)	Q3 2011

Table 5: Summary of milestones for laser system.

2.3 Laser Frequency Noise Suppression

Laser interferometers use the wavelength of the laser light as the yardstick for measuring the displacement of the interferometer arms. A change in the laser wavelength (or equivalently the laser frequency) will be misinterpreted as a change in measured separation of the proof masses; uncorrected frequency noise from free-running lasers would overwhelm the desired sensitivity of the LISA interferometric measurement Conventional Michelson interferometers are operated with nearly equal length arms so that the effect of laser frequency noise cancels when the light from the arms is recombined. Alternatively, locking the laser to a stable length reference, such as an optical cavity, can stabilize the frequency. LISA uses a novel combination of these standard techniques.

LISA laser frequency stabilization is done in two stages, similar to the two-stage process used in ground based gravitational wave detectors. First, the lasers are pre-stabilized to a reference cavity residing on the optical bench. **Pre-stabilization to a reference cavity has demonstrated better than the required frequency stability in laboratory setups at GSFC [20], University of Florida [21], and Hannover [22] several years ago.** In 2007 the GSFC laboratory also demonstrated the frequency tuning capabilities of the cavity pre-stabilization system [23]. By locking variable frequency-offset sidebands to the cavity, tuning was enabled without degrading stability and with no mechanical modifications to the cavity. This tuning is important for LISA's tiered stabilization approach.

The second stage of stabilization locks the laser frequency to the 5 million km LISA arms, which provide an even more stable reference due to the drag free performance and the large separation of the spacecraft. This "arm-locking" will improve laser frequency stability by an additional factor of 100 beyond the cavity pre-stabilized noise level. This master laser stability will be transferred to all other lasers using heterodyne phase locked loops. Arm-locking control algorithms were developed [24] that provide sufficient gain and phase margin to adequately handle the 33 second round-trip delay time of the LISA arms. **These algorithms were successfully validated on several numerical simulations at the Jet Propulsion Laboratory [25][26] and hardware tests at the Albert Einstein Institute [27], University of Florida [28], and the Australian National University [29].** More recent analyses account for all relevant noise sources including USO noise, spacecraft motion, shot noise, and imperfect knowledge of the Doppler frequencies [30].

The final step in frequency noise suppression is a post-processing technique called Time-Delay Interferometry (TDI). TDI is needed because the LISA arms can differ in length by up to 1% over the course of a year due to the natural orbital motions. TDI removes laser frequency noise by forming linear combinations of the phase measurements that are free from laser frequency noise. TDI can be understood as a way to synthesize an interferometer that has equal arm lengths. To achieve this, phase measurements recorded locally at each spacecraft are time shifted using high

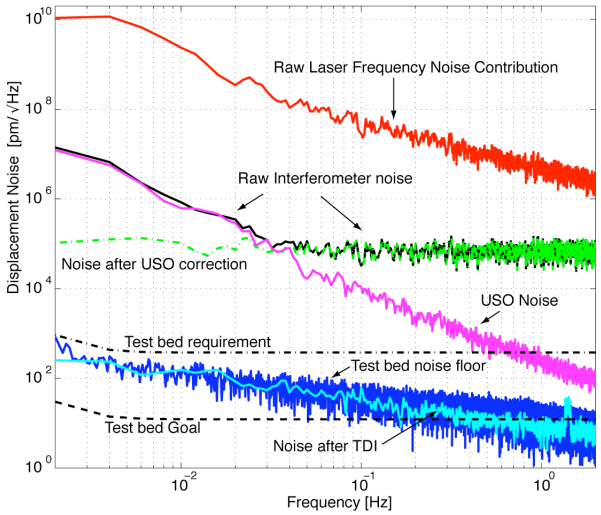

Figure 12 Experimental results from the interferometry test bed showing laser frequency noise suppression. The laser frequency noise is suppressed by combining the phase measurements, correcting for the USO noise, and finally interpolating the measurement to form the TDI combination.

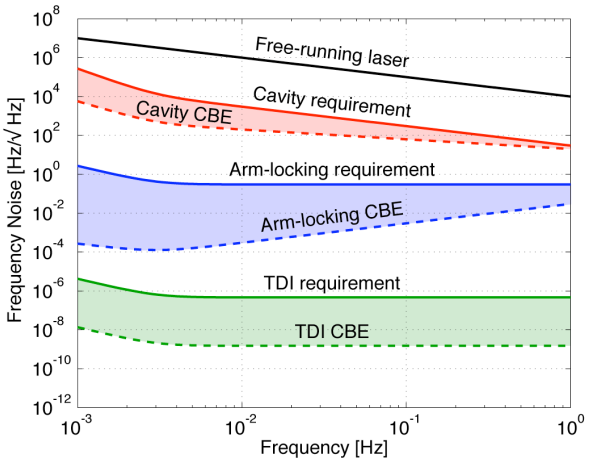

Figure 13: Laser frequency noise vs. signal frequency after each stage of suppression (cavity stabilization, arm-locking and TDI). Solid lines indicate the stability requirement, dashed lines show the current best estimate (CBE) of capabilities, and the shaded areas highlight the margin for each stage.

performance interpolation algorithms and recombined in post-processing. These same linear combinations maintain the gravitational wave signal, as it is contained in the difference of the arms while the laser noise is predominantly common to the arms. TDI was initially validated by analyses [31] and numerical simulations [32]. Frequency noise cancellation was first experimentally demonstrated in 2006 in the LISA interferometry test bed at JPL using a simplified version of TDI. In 2008 the test bed was upgraded to include the complete implementation of TDI, including interpolation and noise from the USOs. **This demonstration [33], performed using the TRL 4 phasemeter, suppressed the laser frequency noise by more than 7 orders of magnitude down to the intrinsic noise floor of the test bed as shown in** Figure 12**.**

A project-wide meeting was held in November, 2008 to refine the design and performance estimates of laser frequency control, including all subsystems: analog and digital electronics, laser prestabilization, arm-locking, and TDI. A white paper detailing this progress is in preparation. A summary of frequency control subsystem requirements and current best estimate is shown in Figure 13, which shows substantial margin in laser frequency noise performance for LISA.

In 2004, the Interferometry Integrated Technical Advisory Team (ITAT), an international team of technical experts in LISA interferometry, listed laser frequency suppression as a top risk, owing largely to the lack at that time of an experimental demonstration of TDI with realistic signal environments. Since that assessment, arm-locking has been included in the baseline design and Time-Delay Interferometry has been shown to meet its requirements with a substantial margin. All components used for these techniques are available in flight qualified versions. The risk has been sufficiently retired to a point where no major developments are required beyond normal spaceflight engineering. Table 6 summarizes the milestones for frequency noise suppression technology development.

Milestone	Date
Cavity sideband locking demonstration	*Completed July, 2007*
Baseline arm locking performance	*Completed April, 2006*
High fidelity arm locking simulation	*Completed Feb, 2009*
Demonstrate minimum-mission performance with laser frequency noise	*Completed Dec, 2006*
Laser frequency noise correction demonstration	*Completed Mar, 2008*
Clock noise correction demonstration	*Completed June, 2008*
TDI demonstration with laser comm. (Interferometer Gate 1)	Sept, 2009

Table 6: Summary of milestones for laser frequency noise suppression.

2.4 Phase Measurement System

The phase measurement system (PMS) extracts displacement information from the optical interference between the received and local laser light. As shown in Figure 14, the PMS consists of a quadrant photoreceiver, an analog-to-digital converter (ADC), a phasemeter for signal processing and an ultra-stable oscillator (USO) reference signal. Of these, only the photoreceiver and phasemeter require technology development, as suitable flight-qualified ADCs and USOs exist that meet the LISA requirements. The photoreceiver converts the optical power into an electrical signal that is digitized by the ADC. The phasemeter processes this digitized electrical signal to extract the phase of the interference. This phase is proportional to relative displacement of the mirrors in the measurement path and contains the gravitational wave strain information.

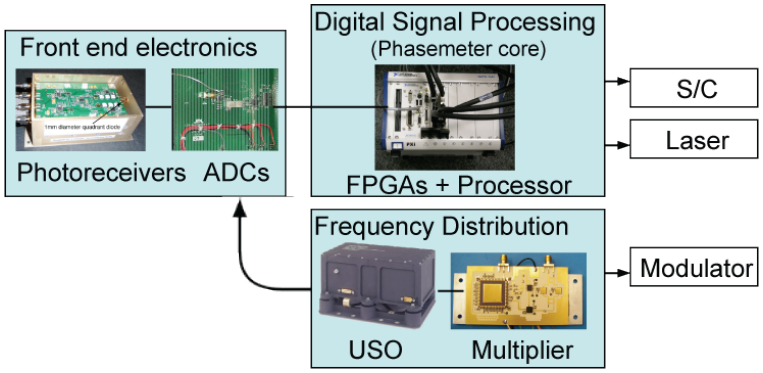

Figure 14: Major components of PMS. The digital signal processing forms the core of the phasemeter. ADC: Analog to digital converter, FPGA: Field Programmable Gate Array, USO: Ultra-stable oscillator, S/C: spacecraft bus.

Two separate TRL 4 photoreceiver designs have demonstrated the primary performance requirements of low noise (13 pW/Hz$^{1/2}$) and relatively high bandwidth (20 MHz) using a quadrant diode with a 1 mm diameter. The photoreceivers convert the optical power of interfering laser beams to a signal voltage to be measured by the phasemeter. The use of a quadrant detector provides both the displacement and pointing measurements required for LISA. The low noise requirement comes from detection of the low signal power received from the distant spacecraft, and the bandwidth requirement is derived from the residual inter-spacecraft Doppler shift for the LISA orbits. A photograph of one of the TRL 4 prototypes along with measured noise performance is shown in Figure 15. The two TRL 4 designs differ in some components choices and the mechanism for separating the DC and AC signal paths.

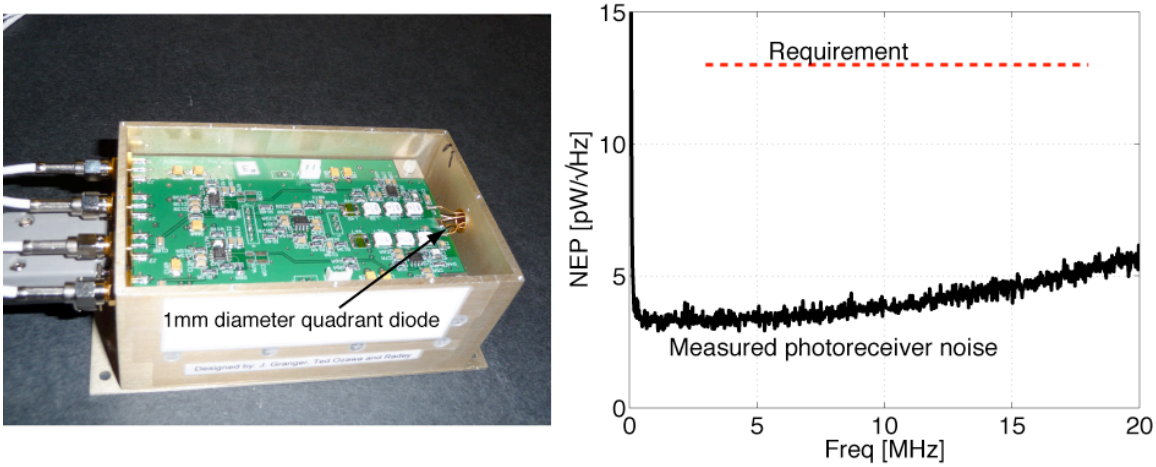

Figure 15: Quadrant photoreceivers (TRL 4) have been developed that meet the primary requirements of low noise and bandwidth (right). NEP: Noise Equivalent Power.

The LISA phasemeter is based on a digital phase-locked loop architecture implemented on a field programmable gate array (FPGA). The most challenging requirement for the phasemeter is measurement linearity, stemming from the need to cancel large amounts of laser frequency noise in post processing. The phasemeter is required to maintain one microcycle/√Hz noise level in the presence of the prestabilized laser frequency noise, a suppression factor of $5x10^{10}$ at 10 mHz. Test results satisfying this linearity requirement are presented in Figure 16, showing that by combining measurements of three signals with correlated phase noise a residual noise of a few microcycle/√Hz is achieved. **The TRL 4 phasemeter developed at JPL [34] achieved a suppression factor greater than $5x10^{13}$ at 10 mHz, 1000 times better than required. The TRL 4 phasemeter also meets LISA's noise and bandwidth requirements and includes auto acquisition, multi-tone measurement, and tracking capabilities [34].** Ranging, clock offset measurement, and communications signal functionalities are currently being implemented, expected completion date September 2009.

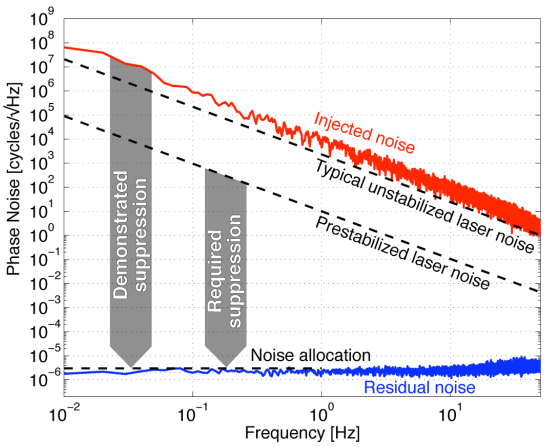

Figure 16: Test of phasemeter linearity combining measurements of three signals with correlated noise. The residual noise in the combined output was suppressed down to the phasemeter design noise floor, with injected noise 1000 times greater than required, (greater than unstabilized, or free-running, laser frequency noise).

A spaceflight architecture study and reference design for the digital signal-processing portion of the TRL 4 phasemeter prototype was completed in January, 2009, satisfying the TRL 5 criteria established in the LISA Technology Development Plan. Xilinx Virtex 5 FPGAs and a Power PC 7447 running Green Hill's Integrity Real-Time Operating System were used to benchmark resource utilization to optimize the FPGA-processor interface for the large number of channels tracked by the phasemeter. The benchmarks use the TRL 4 phasemeter prototype and test equipment to confirm proper functionality of both centralized and distributed processing architectures. In addition to defining the firmware-software interface and baselining a flight architecture this effort resulted in the first bottoms up engineering estimate of mass, power and volume for the digital signal processing portion of the phase measurement system.

Table 7 summarizes the major milestones for PMS. The TRL 4 phasemeter will be used to test the analog and digital signal processing in a system level test of the time-delay interferometry in 2009. These tests will assess the performance of all primary functions of the phasemeter including, laser frequency noise cancellation, clock noise transfer and correction, and weak light phase locking, absolute ranging and laser communication. Other milestones chart the progress of the PMS technology readiness level.

Milestone	Date
Phasemeter breadboard (TRL 4)	*Completed Nov, 2007*
Photoreceiver (TRL4)	*Completed Nov, 2007*
Phasemeter (digital unit) TRL 5 Report	*Completed Jan, 2009*
TDI demonstration with laser comm. (Interferometer Gate 1)	Sept, 2009
Photoreceiver TRL 5	Nov, 2009
Phase measurement system (TRL6)	Dec, 2011

Table 7: Milestones for the Phase Measurement Subsystem.

3 DRS Technologies

The design of the LISA S/C is driven by the need to keep the proof masses as undisturbed as possible. All the elements used for this purpose are grouped together into what is called the Disturbance Reduction System (DRS). The DRS consists of a set of sensors, actuators, and the control laws that bind them together to meet the disturbance and pointing requirements during LISA science operations. It also includes design features, such as thermal and magnetic shields, that are implemented to keep disturbances from reaching the Proof Mass (PM).

The heart of the DRS is the Gravitational Reference Sensor (GRS) which houses the PM. It provides sensing and forcing of the PM position and orientation relative to the spacecraft, along with other functions. Micronewton thrusters provide the actuation for controlling the position and orientation of the spacecraft (S/C). DRS control laws contain loops for drag-free operation as well as pointing the outgoing beams toward the distant S/C.

The top level DRS requirement is that the amplitude spectral density of the PM acceleration disturbance be kept below:

$$\sqrt{S_a} \le 3\times 10^{-15}\sqrt{1+\left(\frac{f}{8mHz}\right)^4}\sqrt{1+\left(\frac{0.1mHz}{f}\right)}\ \mathrm{m/s^2/\sqrt{Hz}}\ ,\ 0.03\ \mathrm{mHz} \le f \le 0.1\ \mathrm{Hz}.$$

A detailed acceleration noise budget was developed that sets the required level of all known disturbance effects [35].

3.1 Gravitational Reference Sensor

The Gravitational Reference Sensor (GRS) is the subsystem that includes [36]

- A 2 kg Au-Pt proof mass (PM) as shown in Figure 17.
- A capacitive readout and an electrostatic actuation system made out of a set of sapphire electrodes completely surrounding the PM. In orbit the PM is fully free floating and it has no mechanical contact of any kind with the surroundings (Figure 17).
- A caging mechanism: a mechanism to hold the test-mass fixed during launch and to release it in free floatation once in orbit (Figure 18).
- An ultraviolet (UV) light charge management system: UV light is shone via a set of optical fibers either onto the PM or onto the electrodes. This generates a photoelectron current whose direction, to the PM or from the PM, is adjusted to keep the PM neutral. Photocurrent direction is adjusted by regulating the balance of illumination between the PM and its surroundings. No voltage bias is needed for this purpose (Figure 18).
- A vacuum chamber that includes the PM, the electrode housing, and the caging mechanism and is evacuated by a set of getter pumps (Figure 19).
- A set of tungsten gravitational compensation mass to suppress the difference of gravitational force between the proof-masses are carried both inside and outside of the vacuum chamber.
- A window in the vacuum enclosure and a hole through the electrode housing to allow reflection of the laser beam onto the PM (Figure 17 and Figure 19). In normal operations the local "short arm" laser interferometer is the main readout of the motion of the PM relative to the spacecraft. This measurement is used both as an element of the PM to PM 5 million kilometer GW measurement, as explained in Figure 6, and as input to the drag-free control. The drag-free control loop, acting on the microthrusters, tries to minimize the variation of the interferometer readout, thus keeping the spacecraft at rest relative to the PM along the direction of the laser beam.

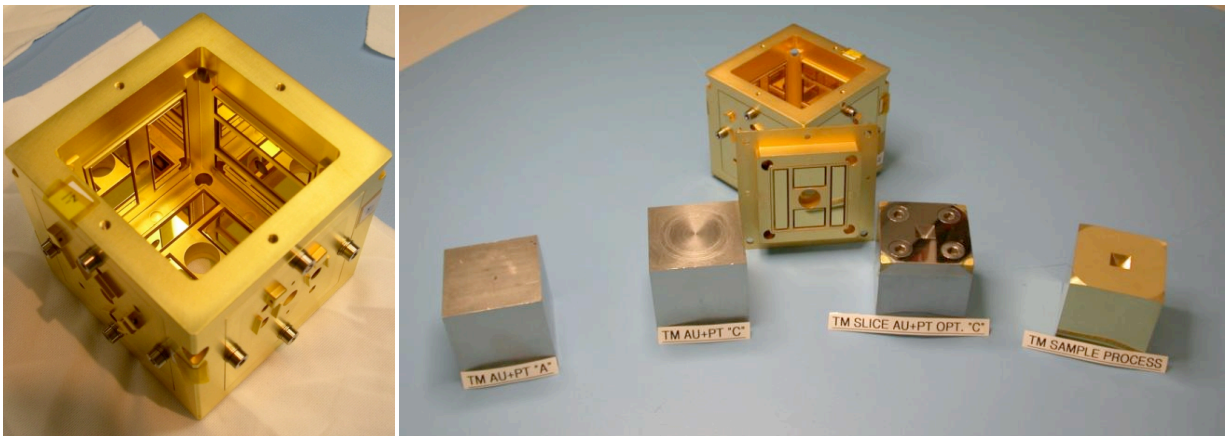

Figure 17: Engineering model of the electrode housing is shown together with examples of the gold platinum PM (bottom from left to right: two flight models before polishing and gold coating. A dummy used for testing of the caging mechanism. A complete model developed to qualify the process).

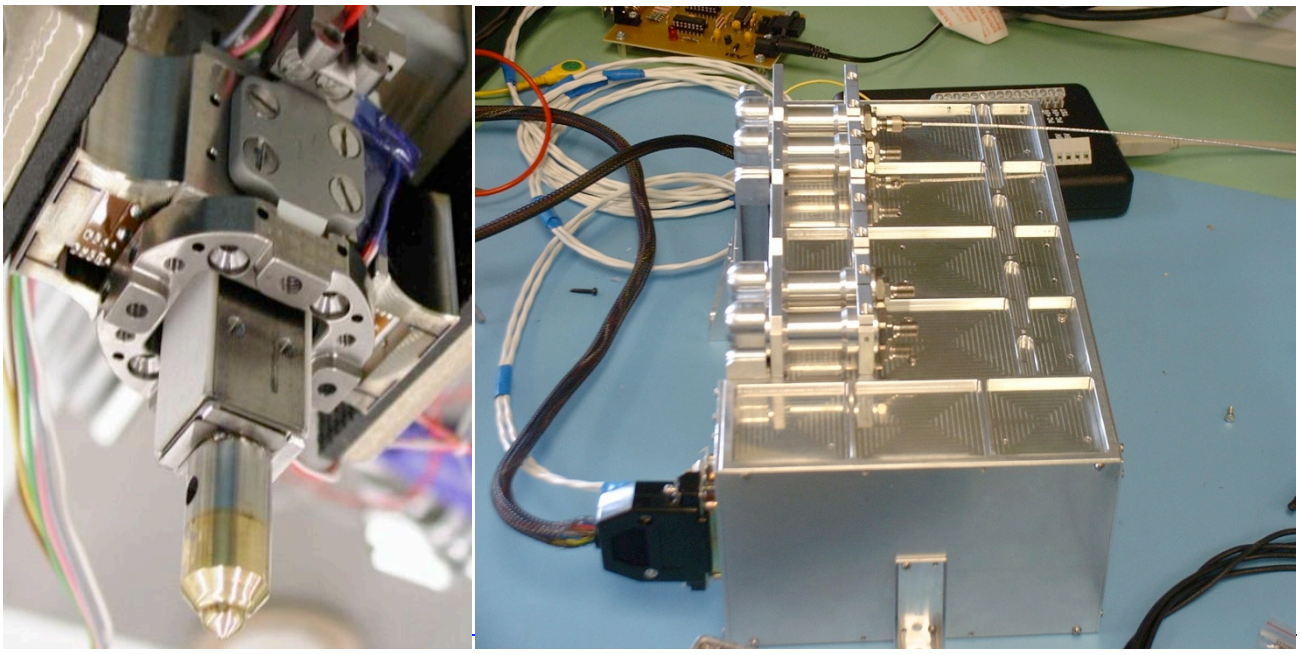

Figure 18: Left: the qualification model of one of the element of the caging mechanism: the central plunger that positions the PM in the center of the housing and then releases it in free flight. Right the qualification model of the UV lamps and their control unit for the charge management device.

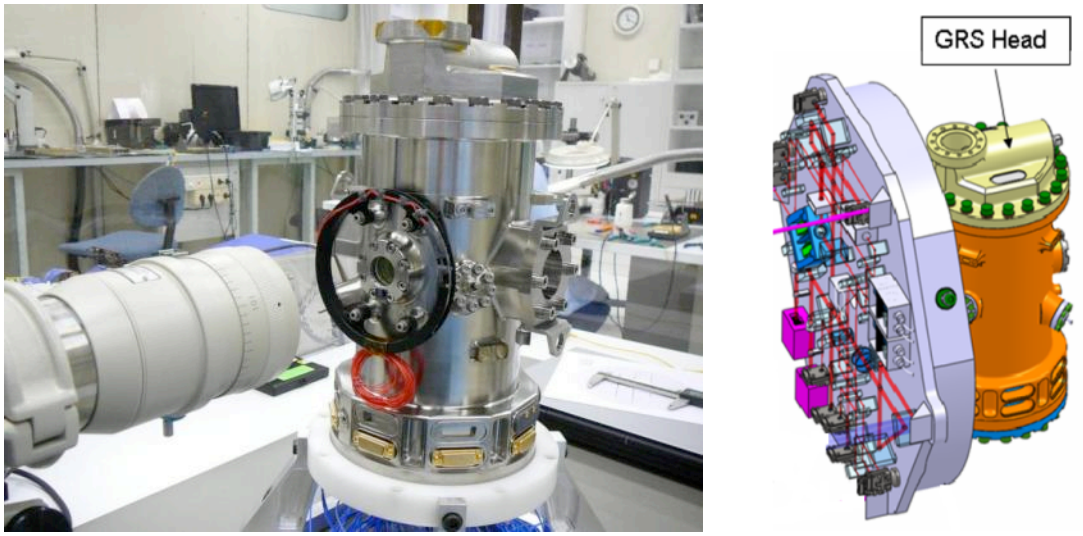

Figure 19: Left: an overall view of the qualification model of the GRS for LISA Pathfinder. The black ring is a magnetic coil used to test in flight the response to magnetic field. In the center of the coil, one of the optical windows used for the laser beam is visible. Right: current design on the interface between the GRS and the LISA optical bench.

The GRS shares some design features with precision space accelerometers (such as the GRACE accelerometer), but differs in a few critical respects. First, capacitive sensing is only used for PM degrees of freedom other than the GW sensitive direction, i.e. the direction of the laser beam. Thus high accuracy readout does not require large electrical fields as is the case instead for capacitive sensing. Second, electrostatic actuation is not used along the sensitive direction. In this direction the spacecraft chases the proof mass.

The PM also has a much weaker coupling to the spacecraft in the GRS than in an accelerometer. This is obtained in various ways. In the GRS there is no mechanical contact of the PM to the

surroundings. On the contrary, in accelerometers a micron-thick wire is used to ground the PM. The gaps separating the PM from the electrodes are much wider in the GRS (3 to 4 mm depending on the direction), than in accelerometer (10-100 μm). This is necessary to keep some of the disturbances well within the requirements. Examples of these disturbances are the natural charge patches on the electrode and PM surfaces, and the impact of the residual gas molecules on the PM. The loss in motion sensitivity of the capacitive readout, resulting from the large gaps, is tolerable as it only affects the less critical non-sensitive directions.

Finally, the GRS is made out of thermal conducting materials, Sapphire for the electrodes and Molybdenum for the housing, as opposed to the high mechanical stability, very low conductance glass-ceramics used in accelerometers. Displacement sensing errors due to thermal distortion, a problem for the high sensitivity capacitive readout of accelerometer, are less important for a GRS than disturbances coming from thermal gradients.

Dedicated developments for the LISA GRS started in 1998. The activity was substantially boosted by the approval of the LISA Pathfinder mission in 2001 and with the beginning of its implementation in 2004. This development consists of two main components:

- The development of a few crucial test methods to demonstrate the basic physical model of the device on ground. This is made mostly by using high fidelity replicas of the GRS, surrounding a PM suspended within a high resolution torsion pendulum(Figure 20)([37][38][39])[37]. **For some of the disturbances the method has now achieved sensitivities within a factor 10 of LISA requirements** (Figure 21)([42][42][46])**.**
- The development of a robust, space qualified flight model to be demonstrated in flight on LISA Pathfinder. **The LISA Pathfinder units are designed to meet all of LISA requirements** ([40][41]). Relaxation of performances relative to LISA are only expected because of the different conditions of operation on board LISA Pathfinder.

Ground testing

A full system level demonstration of the GRS performance on ground is limited because of the 1 g environment. Electric or magnetic levitation of a high density PM is orders of magnitude too noisy to give significant information. The logical route chosen for LISA, as for many spaceflight missions, is to use modeling and analysis anchored to a series of critical experimental tests.

Probably the most relevant set of these tests is the one that has been performed with a torsion pendulum (Figure 20)([37][38][39][42][45][46]). A lightweight PM with the same surface shape and finishing of the high density flight one hangs from the inertial member of a torsion pendulum. The PM is surrounded by a faithful replica of the GRS:, the electrodes, electrode housing, UV charge management system, etc. There is no contact between the PM and the surroundings thus properly imitating the free-floatation condition. In one of the possible configurations, the inertial member is made out of 4 identical PM each at one tip of a cross-shaped structure (Figure 20, top left). One of these proof masses is surrounded by the GRS. As the PM is well off the fiber axis, the torsion motion of the pendulum translates in practice into a linear translation of the PM. In addition, some investigations were also performed with the PM directly hanging from the torsion fiber.

The PM is hollow for these tests to make it light enough so that a thin torsion fiber can be used to maximize the sensitivity of the torsion pendulum. This feature prevents the measurement of volume forces, like gravitation or magnetic, but makes still possible the crucial investigation of surface forces: dc or low frequency electric fields (like those generated by charge patches or by the

back action of the electronics), higher frequency electromagnetic fields (eddy currents due to ac-magnetic field), photon pressure from the laser and thermal infrared radiation, and molecule impact noise (Brownian force or the radiometer force due to temperature gradients fluctuations). All these phenomena have been studied within this realistic GRS model and have confirmed, or contributed to update, the physical model of surface disturbances (Figure 21)([42][44]).

Finally, the residual noise of the pendulum puts an upper limit to any unforeseen surface force noise. This force upper limit, when converted to differential acceleration noise for the 2 kg flight PM, is now at $5\text{x}10^{-14}\text{ms}^{-2}/\sqrt{\text{Hz}}$ at 1 mHz, within a factor two from LISA Pathfinder goal and within a factor ≈10 from LISA requirements at the same frequency (Figure 21)([46]).

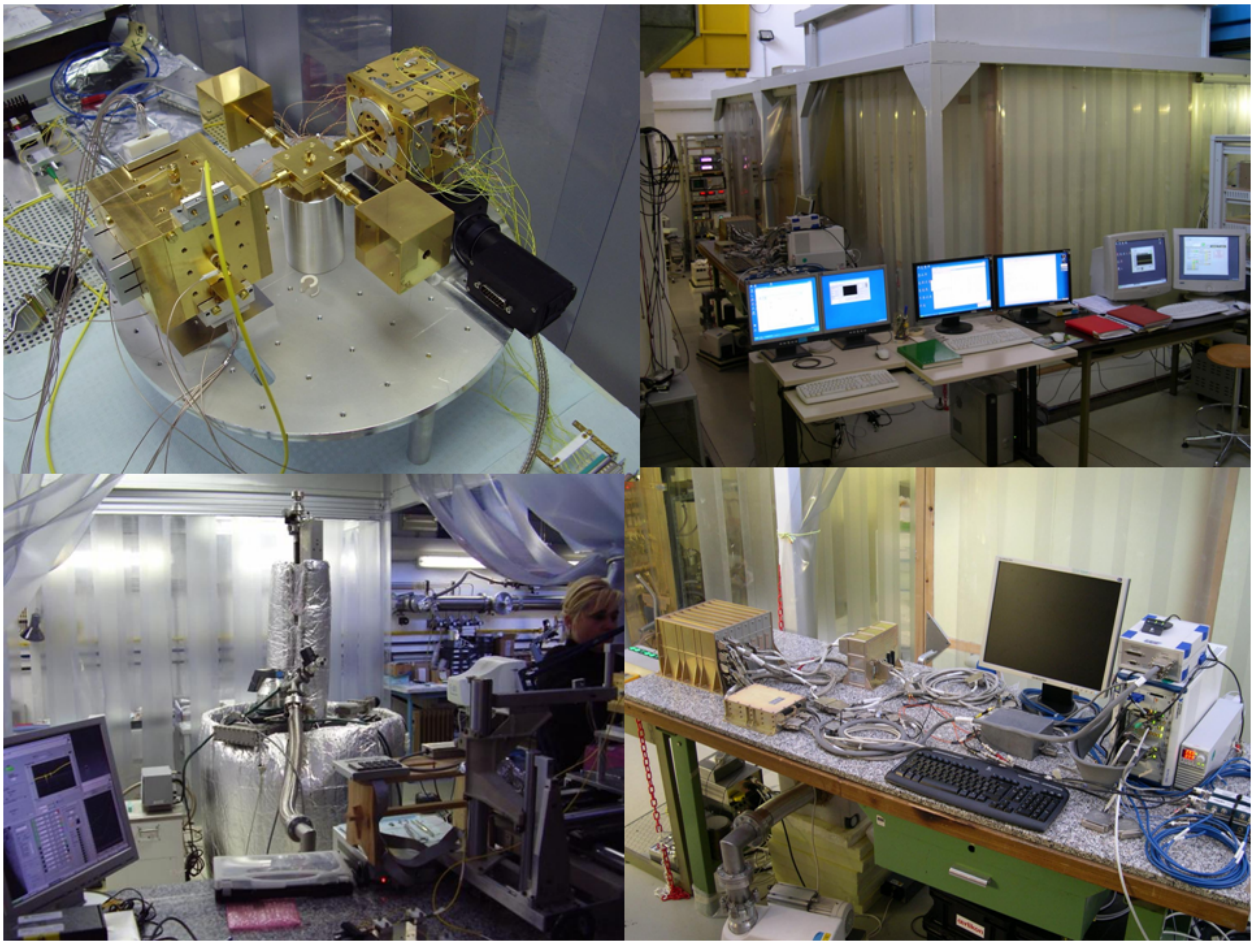

Figure 20: Top left: the inertial member of a LISA torsion pendulum test. The GRS under test is the device on the top-right. A shaft, part of the inertial member, is connected to a cubical hollow PM (not visible) included within the visible electrode housing. On the opposite side of the GRS there is a simplified version of it used for additional sensing of the torsion pendulum motion. Top right: the control console of the pendulum. The pendulum itself is included in the clean room behind the console. Bottom right: the qualification model of the GRS front-end electronics being tested on a GRS qualification model operated within the torsion pendulum facility. Bottom left: the vacuum chamber of the torsion pendulum during assembly within the clean room.

Specialized investigations with a configuration different from that of the flight GRS have also been performed. These investigations where aimed to target some disturbances that are difficult to detect with the full system. For example, ultra-lightweight pendulum was used to verify the level of parasitic voltage fluctuations ([43])(Figure 21, top right). The result of this investigation showed that these fluctuation are well within LISA requirements.

Other tests were performed within the bandwidth required for LISA Pathfinder, including the PM magnetic properties, stability of electrostatic actuation and sensing, and performance of the optical motion readout. All these tests confirmed the disturbance budget of LISA Pathfinder. The results of many of the specific investigations performed so far apply to LISA as well. Radiometer effect, gas damping, charge patches dc potentials, etc. give results largely frequency independent making them relevant to LISA. Some of the studies, like charge patch voltage fluctuations have been performed down to 0.1 mHz and their results then directly apply to LISA.

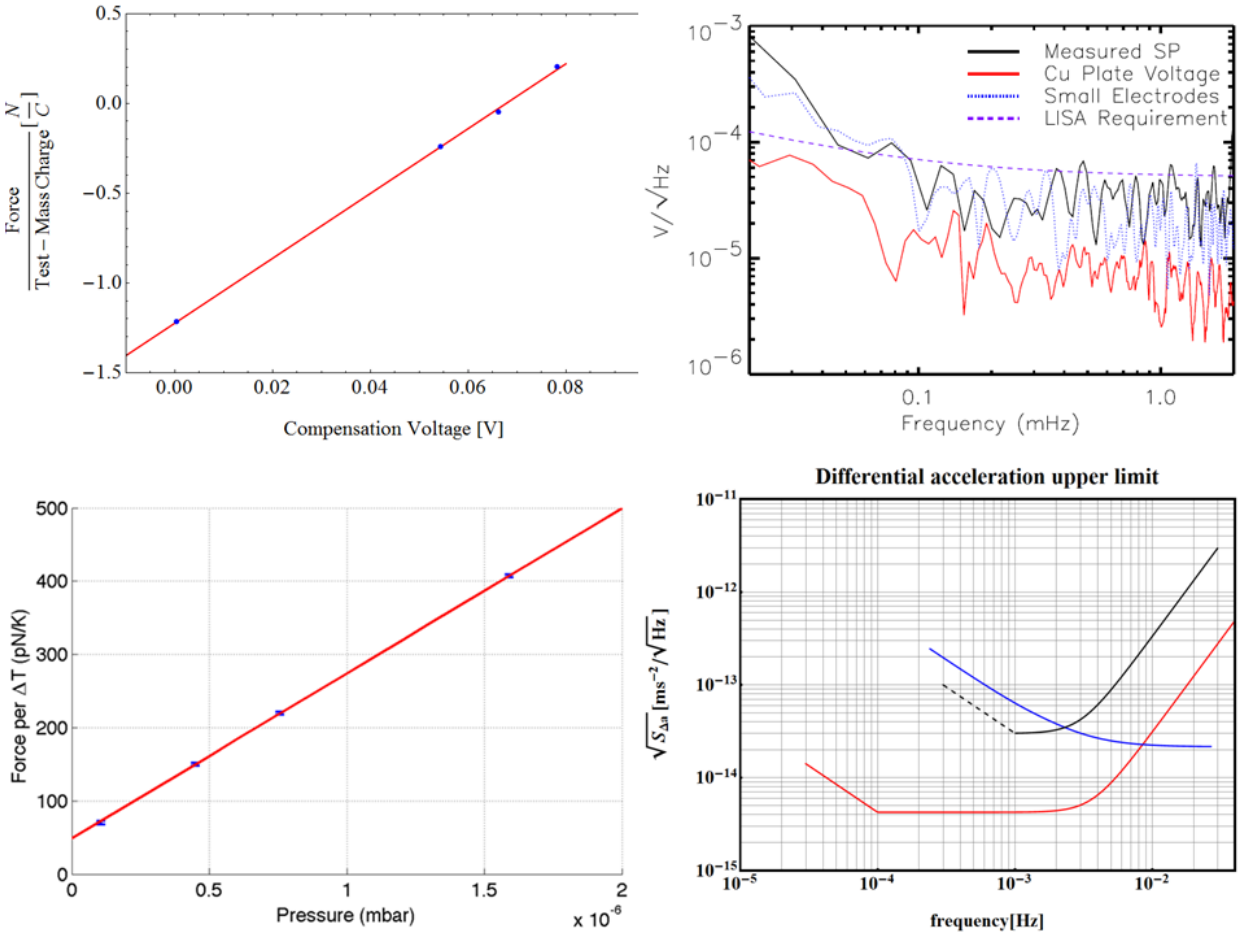

Figure 21: Example of studies with torsion pendulum. Top left: force per unit of test-mass charge as a function of the difference of applied potential (Compensation voltage) across the PM. The non zero force at 0 applied potential shows the effect of parasitic voltage drop due to charge patches on the electrode-housing. The force can be canceled by properly compensating the voltage on the electrodes. In the example shown, the force disappears for a ≈70 mV compensation voltage. Top right: spectrum of parasitic voltage potential fluctuation measured with a special torsion pendulum facility at the University of Washington. Measured fluctuation are compared with the LISA requirements. Bottom left: force per unit temperature drop across the test-mass as a function of pressure for an engineering model of the GRS. The slope of the red line agrees with the prediction of radiometer effect. The zero pressure non-modeled limit is well below LISA requirements. Bottom right. blue line shows the best upper limit on parasitic force as a function of frequency. Data are expressed as an equivalent acceleration noise for a 2 kg LISA test-mass. The red line shows the LISA performance requirement expressed as an equivalent differential acceleration of the two test-masses at the ends of one arm. The black solid line shows the LISA Pathfinder performance requirements, while the black dashed line shows the LISA Pathfinder performance goal.

This long and in-depth test campaign strongly retires the risk that the GRS on LISA Pathfinder may show unpredicted behavior and fall short of the expected performances. However it also constitutes

an important knowledge basis to transform the results of LISA Pathfinder into a comprehensive model of LISA GRS physical behavior.

Development of the flight model

Two complete GRS will be tested on LISA Pathfinder. They are, together with the interferometer, the core constituents of the LTP. These GRS are being designed for use in LISA without major modifications [40].

A full qualification model was developed for all the components of the GRS. Qualification tests were performed for most of the components. The remaining tests and a system level qualification are proceeding while this report is being written (Figure 22). This qualification campaign comes after a long series of partial tests on engineering models of increasing representativeness. Most of the flight hardware components are under manufacturing in parallel with the qualification campaign, as the risk of a major problem is deemed low. The flight models for both GRS will be delivered at the end of 2009.

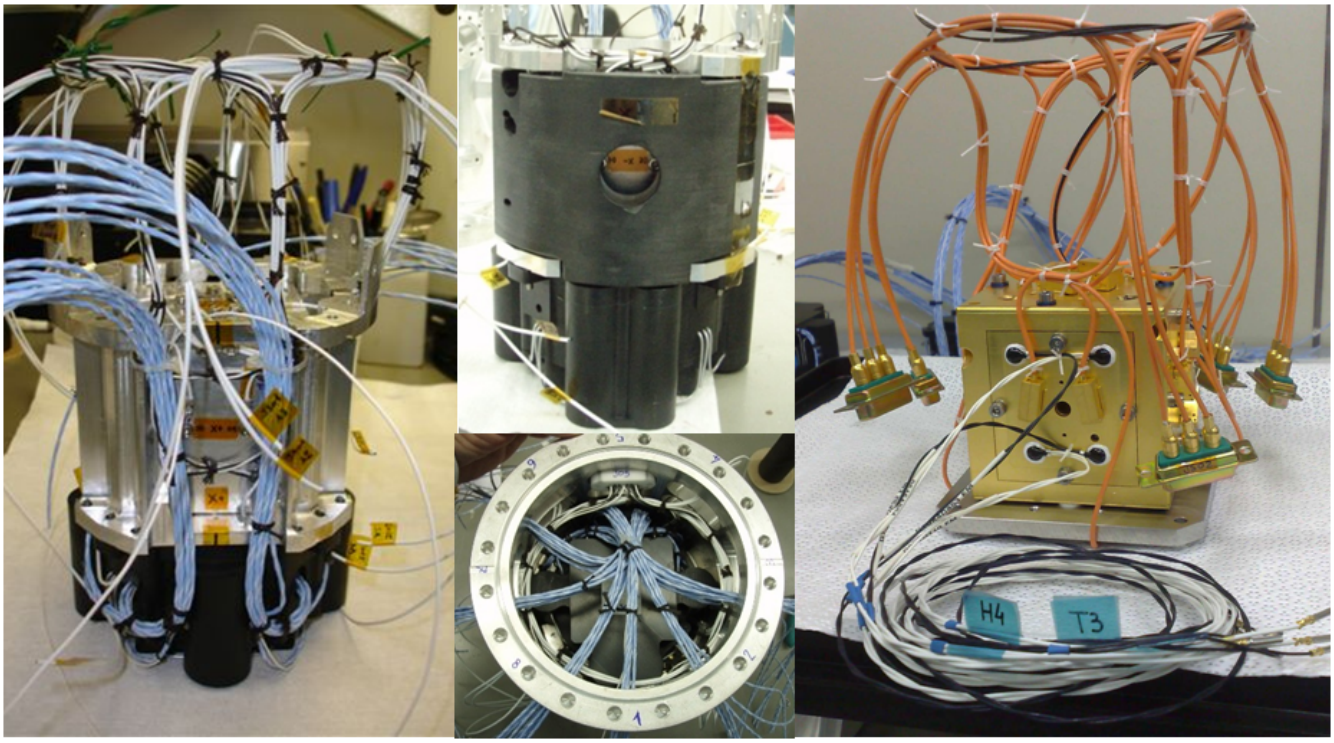

Figure 22: Various phases of the assembly test of the GRS. Left: Routing of the caging mechanism and electrode housing cables. Center top: the gravitational compensation masses integrated onto the central supporting structure. The black device on the bottom is a dummy of one of the caging mechanism motors. Center bottom: the overall assembly inserted within the outer vacuum chamber. Right: the electrode housing qualification model fully wired and ready to be integrated into the torsion pendulum test-bench.

The overall testing campaign has achieved some very important results demonstrating the feasibility of the overall assembly (Figure 22). These include resilience to vibration and thermal cycle, the feasibility of the quite dense packaging of the system, the full performance test of the optical windows, the manufacturability of gravitational compensation masses, functionality and performances of the getter vacuum pumps.

Many features of the GRS flight model can be tested at some level, but only limited system level tests can be performance on ground. The torsion pendulum allows for many tests: unforeseen force

back-action form the front-end electronics, molecular impact noise due to unforeseen anomalous outgassing, anomalous charge patches on the housing, calibration of the charge management system, and calibration of capacitive actuation.

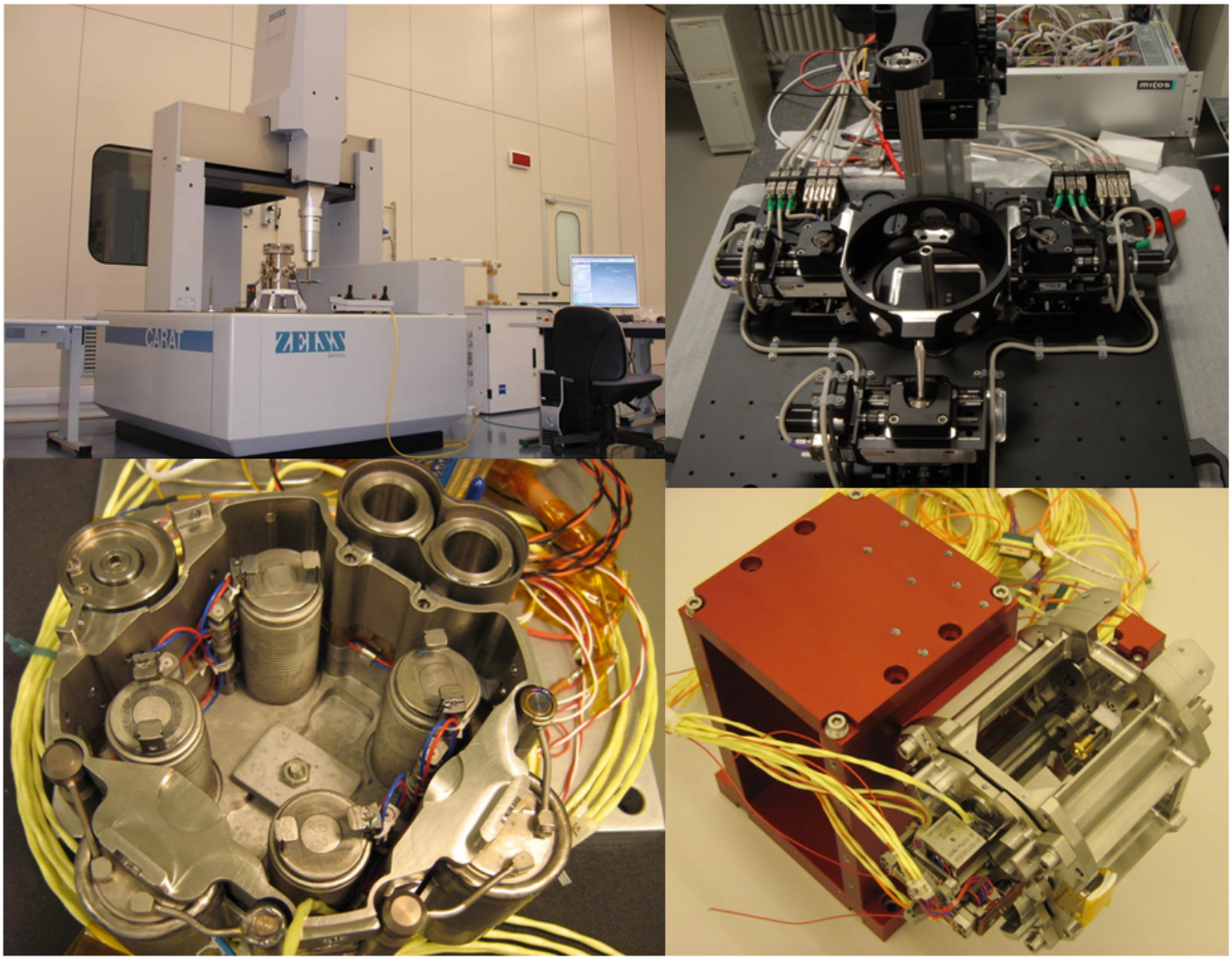

Figure 23: From top left clockwise. The coordinate machine dedicated to the GRS integration. A special hexapod test-bench for calibrating the sensitivity of the capacitive motion readout. The hexapod can displace the flight electrode housing in 6 degrees of freedom around the PM after final integration. The qualification model of the caging mechanism: the central positioning and releasing mechanism assembled onto the central supporting structure. The qualification model of the caging mechanism: the hydraulic motors that actuate the PM launch blocking fingers.

Other tests have and will be performed with other specialized instruments. Calibration of capacitive sensing will be performed at an advance integration stage on a special hexapod device (Figure 23), as it may be sensitive to the details of the cabling. PM magnetic and dynamical properties are tested in specialized laboratories. Also included in the verification plan ([47]) are the more conventional tests: thermal-vacuum, vibration, shock etc. Finally, a series of alignment (Figure 24) and alignment stability tests are performed to integrate it within the rest of the opto-mechanical system.

The development and the performance of this testing plan has a twofold important role. First, it retires risk for LISA Pathfinder. Second, thanks to the nominal equality between LISA and LISA

Pathfinder hardware, it contributes to define and demonstrate the testing plan for LISA, substantially reducing the risk connected to the learning curve about the testing of new technology.

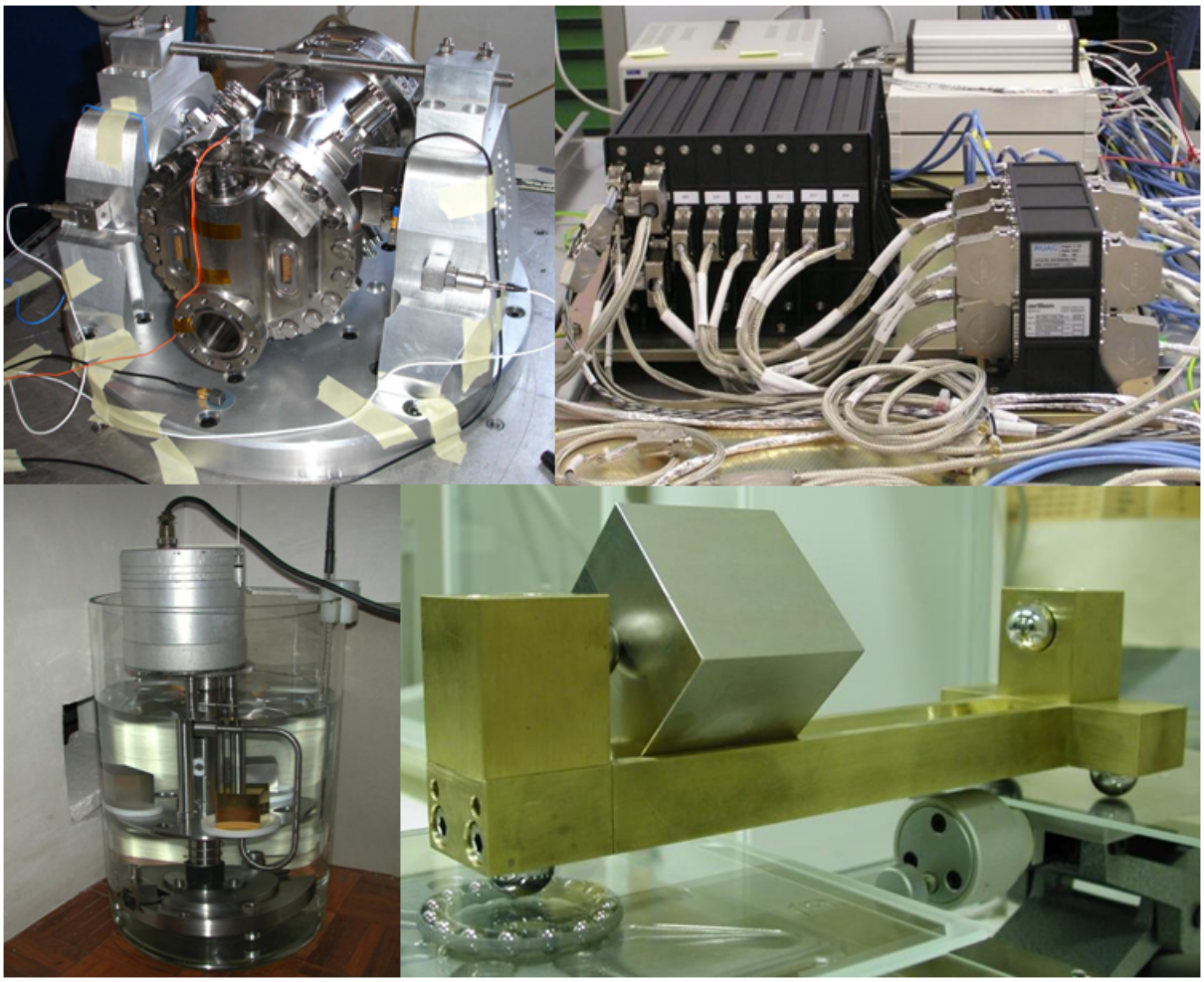

Figure 24: From top left clockwise: Vibration test of the qualification model of the GRS. The qualification model of the front-end electronics. The measurement of the center of mass of the PM. The measurement of the test-mass density.

3.2 Micronewton Thrusters

LISA requires micronewton thrusters to provide the fine spacecraft attitude and position control for drag-free flight and beam pointing to the distant spacecrafts. The thrusters are operated continuously during science measurements with thrust levels set by the disturbance reduction system control loops. Thrust on the order of 10 μN is required to counteract the solar radiation pressure, the largest external force acting on the spacecraft. As shown in Figure 26, the open loop thrust noise must be kept ≤0.1 μN/√Hz above 1 mHz and ≤10 μN/√Hz below 1 mHz in order to prevent disturbances that could influence the proof masses. The key micronewton thruster requirements for the LISA mission are shown in Table 8.

Three different thruster technologies are currently capable of meeting the LISA thrust and thrust noise requirements, and two are being developed to flight readiness in parallel to mitigate risk. In the US, the colloid micronewton thruster (CMNT) made by Busek Co. in Boston have reached TRL 6 by completing all flight hardware fabrication, qualification testing, and I&T activities successfully for ST7 as part of LISA Pathfinder. In Europe, the field emission electric propulsion (FEEP) system is being developed by a team of companies led by Galileo Avionica SpA in Milan, Italy. The European development originally focused on two different thruster technologies for risk reduction: the cesium slit field emission thruster (Slit-FEEP) and the indium liquid metal ion source thruster (Needle-FEEP). The Slit-FEEP thruster will be demonstrated on LISA Pathfinder with flight hardware components currently being fabricated at ALTA SpA in Pisa, Italy (thruster and cluster hardware), Galileo Avionica SpA in Florence, Italy (slit emitter), Astrium SaS in Toulouse, France (cesium tank), and Oerlikon AG in Zurich, Switzerland (thruster lid mechanism). The Needle-FEEP thruster completed engineering model development at ARC in Seibersdorf, Austria (indium ion source) and Astrium GmbH in Lampholdshausen and Friedrichsafen, Germany (thruster and cluster). These thrusters all belong to the category of field emission or electrospray propulsion and will reach TRL 7 after the flight demonstration on LISA Pathfinder.

Parameter	Requirement	Demonstrated	Comments
Thrust Range	Min: 4 μN Max: 30 μN	0.3 to 150 μN	Both Colloid and FEEP thruster emitters can be tailored to meet any thrust range requirement.
Thrust Precision	0.1 μN	0.08 μN	Verified by direct thrust stand measurements and analysis; dictated by bit-resolution of the thruster electronics.
Open Loop Thrust Noise	0.1 μN	See Figure 26	Colloid thrust noise has been verified by direct thrust stand measurements as well (see Ref. [48]).
Science Mode Operational Lifetime	40,000 hours	>3,400 hours	Lifetime has been demonstrated for the LISA Pathfinder mission requirements. Extending the lifetime is the main focus of the remaining technology development program.
Contamination	0.1 μg/cm^2	<0.01 μg/cm^2	Total deposition limit over the lifetime of the mission; demonstrated for LISA Pathfinder mission duration only.

Table 8: Key LISA microthruster performance requirements. All candidate micronewton thrusters have met all of the requirements except thruster lifetime.

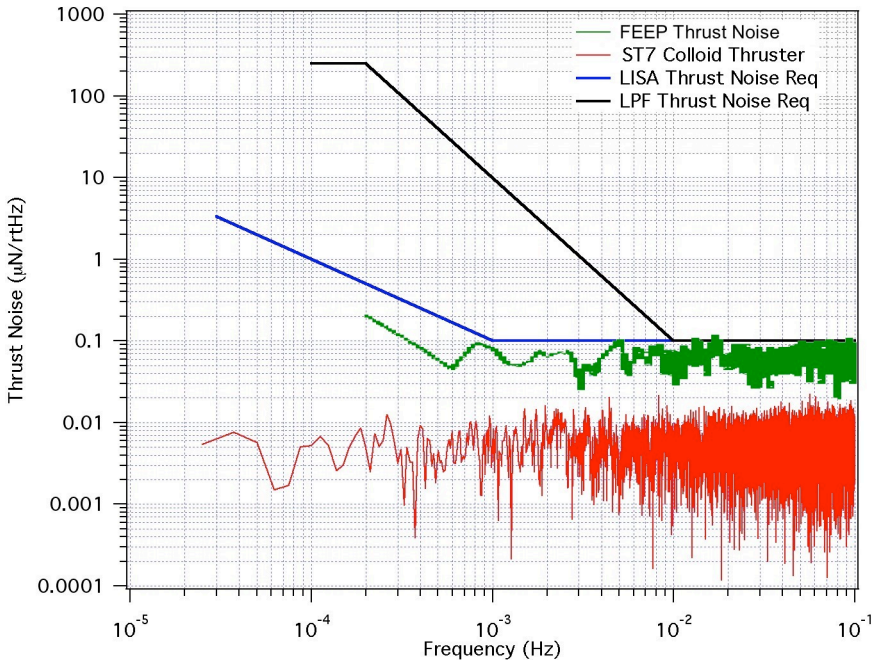

Figure 26: LISA and LPF thrust noise requirements and performance of the Colloid and Slit-FEEP Microthrusters, showing compliance with the requirements.

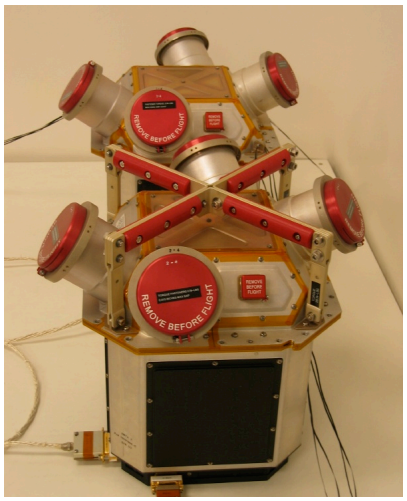

Figure 25: Two flight-ready Busek CMNT clusters have been delivered to JPL for I&T activities on ST7/LISA Pathfinder.

The Busek CMNT development is supported by both LISA and Space Technology 7 (ST7), and will fly on LISA Pathfinder [48]. As shown in Figure 25, two flight clusters, each with four independent thrusters heads, have been delivered to JPL after passing all dynamic and thermal environmental qualification testing. Direct thrust measurements of the CMNT have demonstrated the required thrust noise and resolution, as well as verifying the thrust model used to infer the equivalent thrust from current and voltage measurements. An EM-level CMNT system has also passed through a 3400-hour life test successfully [48]. **The Busek CMNT flight units have completed all integration and test (I&T) activities with the flight avionics unit at JPL and are ready to ship to ESA for ATLO on LISA Pathfinder in the summer of 2009.**

Under LISA Pathfinder, ESA is completing the development on the two types of FEEP thrusters for a wide class of missions that demand steady, high-resolution thrust [49],[50]. Both FEEP thrusters are being specifically designed for LISA Pathfinder to meet the LISA performance requirements. **After completing most of the required development objectives, ESA recently selected the Slit-FEEP technology for flight on LISA Pathfinder.** Development of the Needle-FEEP technology will continue to completion maintaining the technology as a reliable backup for LISA Pathfinder and LISA.

The most recent developments of the Slit-FEEP technology, shown in Figure 27, have focused on completing the Critical Design Review and starting the qualification and flight model manufacturing. After the delivery of the LISA Pathfinder flight hardware, the technology "delta-development" activities specific to LISA will begin in earnest and focus on extending the lifetime of

the FEEP thrusters. Similar to the CMNT, these thrusters have also demonstrated the required thrust noise and resolution (a direct thrust measurement campaign is ongoing to validate ion beam data), and have performed endurance testing in excess of 800 Ns in over 3000 hours of operation.

Figure 27: EM version of a cesium Slit-FEEP thruster for LISA Pathfinder. The Slit-FEEP is also the baseline for the CNES/ESA MICROSCOPE Mission.

Extending thruster lifetime is the most critical development activity for LISA since the thrusters must operate continuously during science measurements, approximately 40000 hours of operation. In the last three years, all three candidate technologies have accumulated over 50000 hours of operation with multiple thruster units in multiple 3000-hour class tests designed around the 90-day LISA Pathfinder mission duration and total impulse requirements. These wear-tests have helped to identify, develop, and verify comprehensive physics-based models of various failure modes and gradual wear mechanisms. Identifying and eliminating failure mechanisms by understanding the physics of the failure modes is critical to demonstrating the LISA lifetime requirement as multiple multi-year class tests with flight-like hardware are not cost effective or possible this early in the LISA project. While a complete long duration test of a LISA microthruster will be conducted, in the near future accelerated testing of LISA Pathfinder thrusters will provide additional data to predict lifetime based on known failure modes.

The key lifetime limiting mechanisms for all the candidate thruster technologies are 1) the gradual deposition of condensable propellant on the electrodes leading to arcing and formation of high-impedance paths that can negatively affect performance, 2) contamination or clogging of the propellant feed system that can have minimum dimensions on the order of 1-10 μm, and 3) erosion of the electrodes. On the first issue, detailed measurements of plume properties (current density, ion energy, plasma potential, etc.) have been used to develop and verify models of ion and charged droplet trajectories. The models and measurements are used to set operating parameters and design electrodes that focus the exhaust beam, reducing overspray (charged particles impinging on electrodes) and the possibility of spacecraft contamination to acceptable levels. LISA Pathfinder will also have on board in-flight diagnostics to measure the spacecraft contamination and plasma effects. On the second issue, extreme care has been taken to develop processes that eliminate contamination and the possibility of clogging inside each of the candidate thruster's propellant feed systems. On the third issue, electrode wear processes are well understood and characterized. Materials have been chosen and electrodes have been designed to reduce erosion rates to acceptable levels for the LISA mission duration. In addition, stringent acceptance criteria have been established for each thruster component to ensure reliability and eliminate "infant mortality" issues as much as possible. While each system has specific challenges in this regard, these issues have been addressed in the ST7 and LISA Pathfinder developments, and LISA will use the same techniques to be demonstrated on LISA Pathfinder. **There are no known lifetime limiting mechanisms that would preclude either of the microthruster technologies from meeting the LISA lifetime requirement.**

In summary, LISA Microthruster technology development has the following objectives:

1. Demonstrate through design, analysis and testing, approaches and requirements that eliminate non-wear-out failure modes found during ST7 and LISA Pathfinder.
2. Identify all critical wear-out failure modes, including those already known and found through accelerated component-level testing of ST7 and LISA Pathfinder hardware.
3. Develop physics-based models of the critical life-limiting processes.
4. Verify, validate and reduce the uncertainty in the life models through predictions and comparisons to accelerated component-level and long-term system-level testing.
5. Identify and implement design changes, only as necessary, to create a LISA prototype thruster that is expected to meet the LISA lifetime requirement.
6. Demonstrate that the LISA prototype thruster design meets all the performance and contamination requirements without introducing new failure modes.
7. Initiate a long-duration lifetime demonstration of the LISA prototype thruster that shows, using test results and verified models, the thruster meets the LISA lifetime requirement.

To accomplish these objectives, accelerated wear-tests and verified models of the identified failure modes will be used to design a LISA prototype microthruster system in 2010. A flight-like CMNT thruster system will be tested to at least 8000 hours of operation by the end of 2011, and 20000 hours by the microthruster Preliminary Design Review (PDR). The LISA project will likely elect to continue the wear test with the same hardware through a full mission duration demonstration of 40000 hours plus margin. A flight-like FEEP thruster system will also begin long duration testing by the end of 2010 in a dedicated LISA lifetime test to cover the full life requirement with margin. It is important to note that for both systems, the flight units will be designed with complete redundancy to insure a successful mission. Key milestones for the micronewton thruster technology development are given in Table 9.

Milestone	**Date**
Complete 3400-hr life test of ST7 EM colloid thruster system	*Nov 2006, Completed*
Complete 3000-hr wear test of 6 independent LISA breadboard colloid thruster systems to identify failure mechanisms	*Sept 2007, Completed*
Demonstrate Micronewton Thruster Performance	*Nov 2007, Completed*
Delivery of Flight-Qualified ST7 CMNT Clusters	*May 2008, Completed*
Complete accelerated testing of ST7 CMNT thruster design	September 2009
Delivery of Flight-Qualified LISA Pathfinder FEEP Flight Units	April 2010
Complete CMNT LISA prototype (PM) microthruster design	April 2010
Complete FEEP LISA prototype (PM) microthruster design	September 2010
Begin long-duration wear test of both CMNT and FEEP LISA prototype microthrusters	October 2010
Complete performance measurements of LISA PM microthrusters	April 2011
Milestone for 8000 hours of PM wear test	December 2011
Milestone for 20000 hours of PM wear test	PDR
Milestone for 40000 hours (plus margin) of PM wear test	CDR

Table 9: Key milestones for the micronewton thruster technology development program.

3.3 Pointing Mechanisms

LISA requires two mechanisms to precisely point the incoming and outgoing laser beams and adjust for the natural orbital motions. In the current baseline, the incoming beam of one telescope is pointed by adjusting the three-axis attitude of the spacecraft with the micronewton thrusters while the other telescope is pointed using a mechanism that steers in-plane the whole optical assembly maintaining the light from the distant spacecraft within the field of view. This mechanism is often referred to as the Optical Assembly Tracking Mechanism (OATM). Each optical bench also contains a mechanized optical element called the Point Ahead Angle Mechanism (PAAM) that is used to steer the outgoing beam. All these actuators are commanded by the disturbance reduction system control loops that use the interferometric differential wavefront sensing and an orbital lookup table as inputs. No mechanism angle encoders are required during science operations.

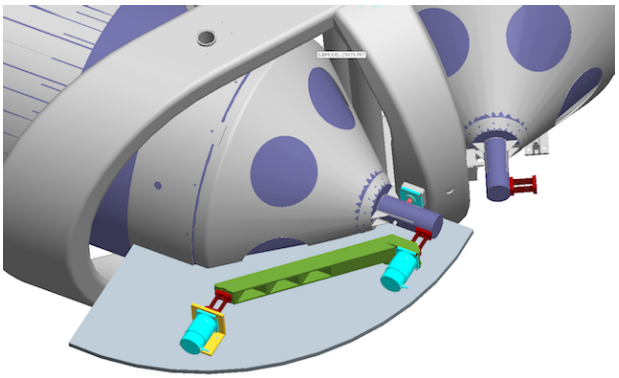

Figure 28: A two stage lever arm system was developed for the optical assembly articulation that uses existing actuator technology.

Quantity	Requirement
Full Pointing Range	± 1.5°
Fine Pointing Rate	5.2 nrad/s
Pointing Jitter (in loop)	1 nrad/√Hz
Digital Control Induced Jitter	0.3 nrad/√Hz
Assembly jitter (in loop)	1 nrad/√Hz, 100 pm//√Hz

Table 10: Driving requirement for the OATM. A testbed is currently under development at GSFC to verify that the lever arm design meets these requirements.

Steering the entire optical assembly avoids coupling spacecraft motion into the pathlength science measurement; all the optical elements move together so there is no induced relative displacement between them. Pointing jitter (from both the OATM and the spacecraft) only enters the measurement through a second order effect driven by the wavefront quality in the far field. The driving requirements of the OATM are shown in Table 10.

A lever arm design was developed to articulate the optical assembly that uses two linear actuators to provide fine and coarse pointing [51]. **The requirements on range and resolution for these actuators are well within the capabilities of commercially available mechanisms, so no technology development is required for this design.** Recently, Physik Instrumente GmbH developed the Nexline linear actuator that appears to have sufficient range and resolution to eliminate the fine stage in this design. A version of this mechanism has already been space qualified for use in the LISA Pathfinder proof mass caging system. The development of a testbed at GSFC is currently underway that will validate the performance of this actuator as well as the overall system design. ESA is

Figure 29: The performance of space qualified Nexline actuator from Physik Instrumente may be good enough to eliminate one of the stages in the lever arm design.

also starting a development activity to look at various options for the OATM. Key milestones for these efforts are given in Table 11.

Unlike the optical assembly articulation, the Point Ahead Angle Mechanism (PAAM) motion enters directly into the science measurement, so it requires an ultrastable design where the optical pathlength is not susceptible to changes at the picometer level. Any dimensional change due to the actuator jitter, misalignment, miss-positioning, thermal gradients, mechanical stress etc. will be seen as a pathlength change in the interferometer output. Fortunately, the rotation rate of this element is very slow as it varies sinusoidally with a one year period, so most of the motion will be out of band. The longitudinal stability requirement is shown in Figure 30.

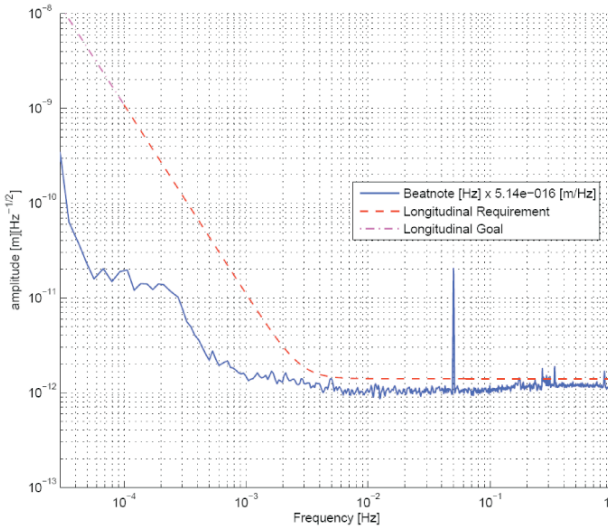

Figure 30: The measured stability of the TNO breadboard PAAM meets the LISA requirements.

Ideally, the PAA is operated continuously for optimal optical performance. However, the rate of change in the point ahead angle is small enough that an operational mode requiring only intermittent adjustment is possible. Small data gaps would likely be introduced every time the angle is adjusted, but these events can be timed to coincide with other scheduled activities that also introduce errors.

ESA is supporting two independent activities to develop, test and validate a breadboard of the PAAM, one with TNO featuring a continuously operated mechanism and the other with RUAG and CSEM designing instead a stepped mechanism. Final results of these activities are expected in July 2009. Preliminary results for the TNO mechanism are shown in Figure 30 verifying that the pathlength stability requirement is already met (note the peak at 50 mHz is due to testing conditions). Key milestones for these efforts are given in Table 11.

Milestone	Date
Kickoff of NASA OATM Testbed Development	*Completed, September 2008*
NASA OATM Preliminary Actuator Testing Complete	June 2009
NASA OATM Testbed Complete	August 2009
NASA OATM Breadboard Study Final Review	December 2009
ESA Kickoff of OATM Activities	*Sept 2009*
ESA Kickoff of PAAM Activities	*Completed, May 2007*
PAAM Design Review (TNO/RUAG)	*Completed Oct 2008 / Feb 2009*
PAAM Test Readiness Review (TNO/RUAG)	*Completed Dec 2008 / May 2009*
PAAM Breadboard Study Final Review	*July 2009*

Table 11: Key milestones for the pointing mechanism technology development.

3.4 Disturbance Reduction System Controls

The Disturbance Reduction System (DRS) controls are responsible for ensuring that the residual acceleration of the two proof masses fall below the LISA sensitivity requirements by providing tight pointing and translational control of the LISA spacecraft and its proof masses. A block diagram illustrating the various loop of the DRS is provided in Figure 1. Although drag free control was used in a number of previous missions, including the Triad drag-free demonstration [52] and Gravity Probe-B [53], it was originally believed that some aspects of the LISA control design were high risk and required technology development. However, control strategies and designs have matured over the course of the past few years and have demonstrated that **standard control systems are capable of meeting the LISA requirements [54][55][56]**. In addition, it was shown that the control system for each spacecraft can be made autonomous and does not require real-time interaction with other spacecraft.

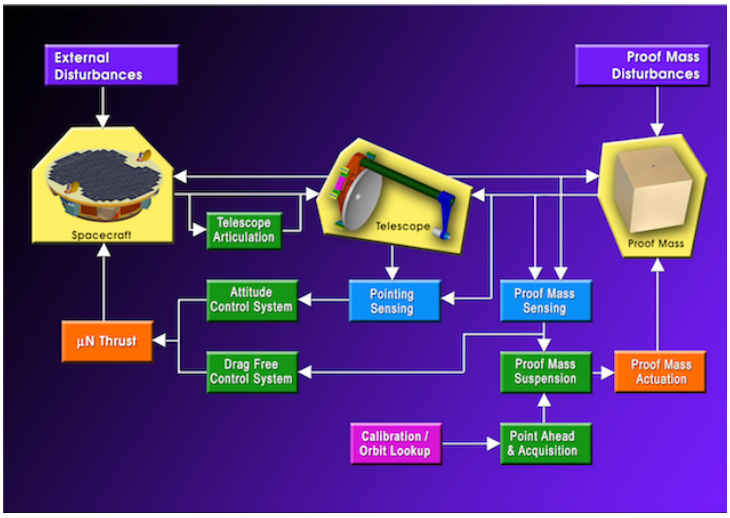

Figure 31: Block Diagram of LISA Disturbance Reduction System. DRS control functions are in green.

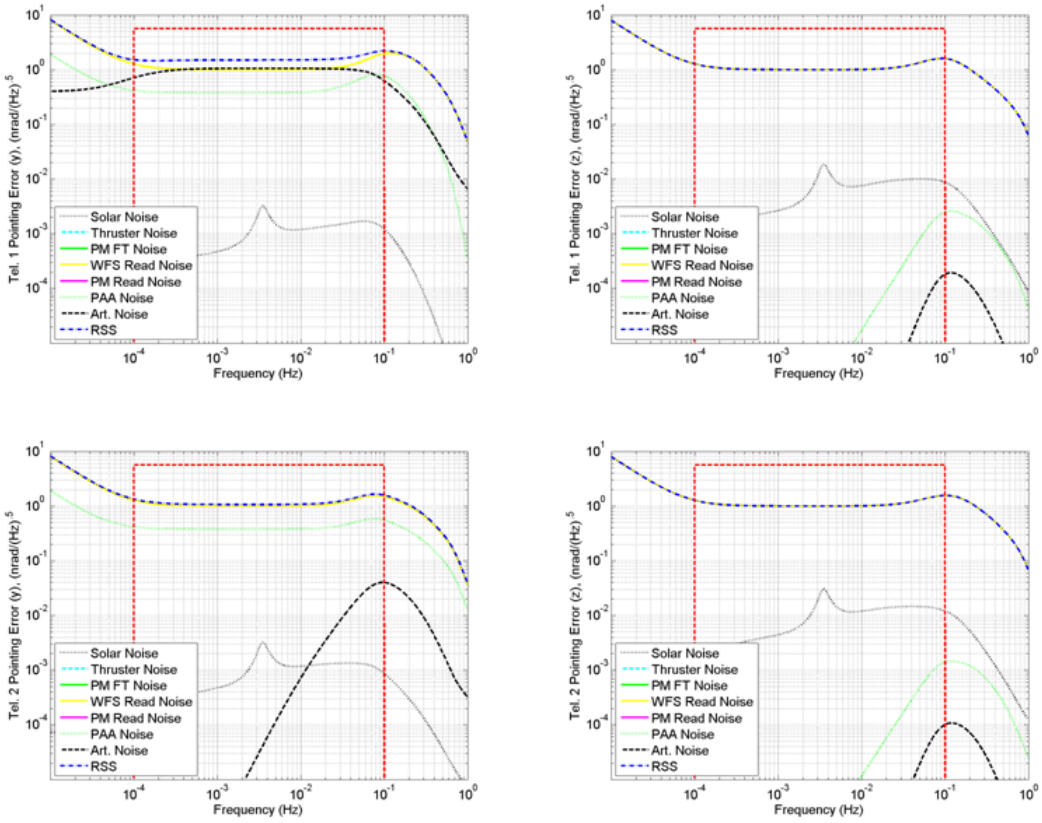

Figure 32: Telescope Pointing Performance for the Arms of a LISA Spacecraft.

Independent designs for DRS Controls were completed by NASA and ESA, and have demonstrated that all DRS requirements can be met with ample margins. Figure 32 and Figure 33 illustrate telescope pointing and drag-free performance of the current designs vs. requirements for a typical LISA spacecraft.

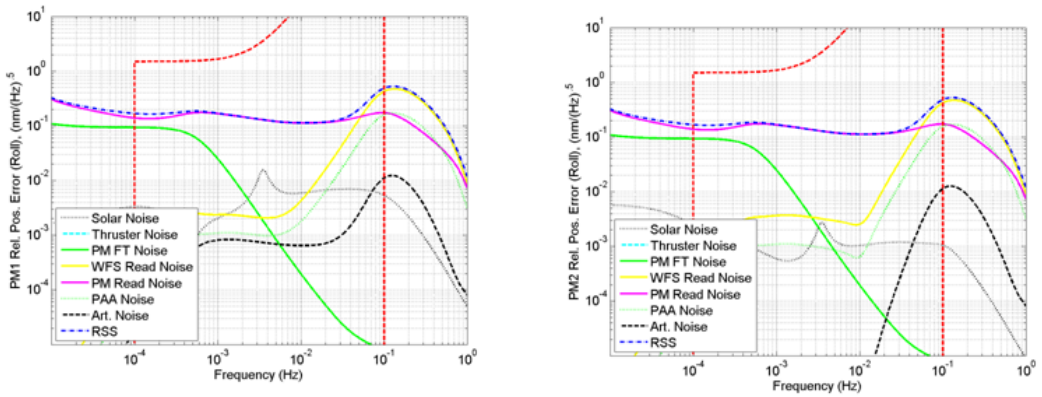

Figure 33: Drag-Free Performance along the Sensitive Axes.

Two strategies for the optical acquisition of the constellation were developed and verified through simulations. Linear and nonlinear models of varying fidelity and complexity, including a high fidelity 57 degrees of freedom model of the LISA constellation, were developed and used in the design and analysis. **The conclusion was that DRS Controls and acquisition can be treated as an application of existing technology [57][58][59][60].**

LISA Pathfinder will demonstrate the general concepts of DRS control. Independently developed DRS control strategies have also been developed by NASA and ESA for Pathfinder [61][62][63][64]. In many ways, the DRS Controls for Pathfinder is more demanding and complex than that required for LISA, mostly because the two proof masses have the same sensitive axis. Hence, this experiment will serve as a good validation tool for LISA DRS controls. The Pathfinder projects will assess the validity of the design and analysis models, as well as their assumptions. It will also assess LISA specific issues, such as impact of charge management, effects of low-level DC field variations in proof mass suspension, performance of a LISA-like gyro mode, and others.

There are no known risks for LISA DRS controls from an algorithmic perspective at this stage of development. However, this is based on the Pathfinder sensors and micronewton propulsion system performing close to their design specifications. The current control designs carry significant margins, which may be used to relax requirements on the hardware at specific frequency bands if necessary.

4 References

[1] "LISA Technology Status Report," LISA Project internal report number LISA-GSFC-TN-430 (February 2007).

[2] "LISA Technology Development Plan," NASA internal report (February 2005).

[3] "Payload Preliminary Design Description," LISA Project internal report number LISA-MSE-DD-0001 (2009).

[4] "LISA Spacecraft Description," LISA Project internal report number LISA-SC-DD-0001 (2009).

[5] LISA NASA-ESA Letter of Agreement (2003).

[6] R. Howard and S. Volonte, "LISA Project Agreement," (August, 2004).

[7] "Science Requirements and Top-level Architecture Definition for the LISA Test-flight Package (LTP) on Board LISA Path Finder (SMART-2)," University of Trento internal report number LTPA-UTN-ScRD-Iss003-Rev1 (June 2005).

[8] http://www.us.schott.com/optics_devices/english/products/zerodur/index.html

[9] http://www.corning.com/docs/specialtymaterials/pisheets/UleBro91106.pdf.

[10] H. Peabody and S. M. Merkowitz, "Low Frequency Thermal Performance of the LISA Sciencecraft," in Proceedings of the 6th International LISA Symposium, edited by S. M. Merkowitz and J. Livas (American Institute of Physics Conference Proceedings, New York, 2006).

[11] G. Heinzel *et al.*, "Components for the LISA local interferometry," in Proceedings of the 6th International LISA Symposium, edited by S. M. Merkowitz and J. Livas (American Institute of Physics Conference Proceedings, New York, 2006).

[12] A. F. Garcia Marin *et al.*, "Interferometric characterization of the optical window for LISA Pathfinder and LISA," in Proceedings of the 6th International LISA Symposium, edited by S. M. Merkowitz and J. Livas (American Institute of Physics Conference Proceedings, New York, 2006).

[13] D. Weise *et al.*, "Optical Design of the LISA Interferometric Metrology System," in Proceedings of the 6th International LISA Symposium, edited by S. M. Merkowitz and J. Livas (American Institute of Physics Conference Proceedings, New York, 2006).

[14] http://www.us.schott.com/optics_devices/english/products/zerodur/index.html

[15] see for example http://www.corning.com/docs/specialtymaterials/pisheets/UleBro91106.pdf.

[16] H. Peabody and S. M. Merkowitz, "Low Frequency Thermal Performance of the LISA Sciencecraft," in Proceedings of the 6th International LISA Symposium, edited by S. M. Merkowitz and J. Livas (American Institute of Physics Conference Proceedings, New York, 2006).

[17] D. Weise, "Laser Subsystem Specification," EADS Astrium GmbH internal report number LISA-ASD-RS-3400 (May 2008).

[18] M Tröbs, S Barke, J Möbius, M Engelbrecht, D Kracht, L d'Arcio, G Heinzel and K Danzmann, "Lasers for LISA: overview and phase characteristics" submitted to Journal of Physics Conference Series.

[19] Simon Barke, Michael Tröbs, Benjamin Sheard, Gerhard Heinzel,Karsten Danzmann, "Phase noise contribution of EOMs and HF cables", submitted to Journal of Physics Conference Series.

[20] G. Mueller, I. Thorpe, J. Camp, & P. McNamara "Frequency Stabilization for LISA" NASA Technical Publications, NASA/TM-2005-212794 (2005).

[21] Rachel J Cruz et al, "The LISA benchtop simulator at the University of Florida," Classical & Quantum Grav. 23 S751-S760 (2006).
[22] Peterseim M, Brozek OS, Danzmann K, et al. "Laser development and laser stabilisation for the space-borne gravitational wave detector LISA," 2nd International LISA Symposium on the Detection and Observation of Gravitational Waves in Space, JUL, 1998 Pasadena CA, AIP CONFERENCE PROCEEDINGS 456 148-155 (1998).
[23] J. Thorpe, K. Numata, & J. Livas, "Laser frequency stabilization and control through offset sideband locking to optical cavities" Optics Express 16 15980-15990 (2008).
[24] B.S. Sheard, M.B. Gray, D.E. McClelland and D.A. Shaddock "Laser frequency stabilization by locking to a LISA arm," Physics Lett. A 320 9-21 (2003).
[25] J. Sylvestre "Simulations of laser locking to a LISA arm," Phys. Rev. D 70 102002 (2004).
[26] A. Sutton and D.A. Shaddock, "Laser frequency Stabilization by dual arm locking for LISA," Phys. Rev. D 78 082001 (2008).
[27] A. F. G. Marín, G. Heinzel, R. Schilling, A. Rüdiger, V. Wand, F. Steier, F. G. Cervantes, A. Weidner, O. Jennrich, F. J. M. Meca et al., Class. Quantum Grav. 22 S235 (2005).
[28] J. I. Thorpe and G. Mueller, Phys. Lett. A 342, 199 (2005).
[29] B.S. Sheard, M.B. Gray, DA Shaddock, D.E. McClelland, "Laser frequency noise suppression by arm-locking in LISA: progress towards a bench-top demonstration," Class. Quantum Grav. 22 S221-S226 (2005).
[30] K. McKenzie, R. Spero, and D. Shaddock, "Arm Locking Performance in LISA," in preparation.
[31] M. Tinto and S.V. Dhurandhar "Time-Delay Interferometry," Living Rev. Relativity 8 (2005). http://www.livingreviews.org/lrr-2005-4
[32] M. Vallisneri, "Synthetic LISA: Simulating time delay interferometry in a model LISA" Phys. Rev. D 71, 022001 (2005).
[33] G. de Vine, K. McKenzie, D.A. Shaddock, R.E. Spero, B. Ware and W. Klipstein "Experimental demonstration of time-delay interferometry," Presentation at the 7th International LISA Symposium, Barcelona June (2008).
[34] D.A. Shaddock, B. Ware, R.E. Spero and W. Klipstein, "Phasemeter TRL 4 technical report". LISA Project LIMAS2007-002 (2007).
[35] DRS ITAT, "LISA DRS Acceleration Noise Budget," LISA Project internal report (January 2005).
[36] "Position sensors for LISA Drag Free control" W.J. Weber et al., Class. Quantum Grav. 19 (2002) 1751–1756
[37] "Torsion pendulum facility for ground testing of gravitational sensors for LISA" M. Hueller et al., Class. Quantum Grav. 19 (2002) 1757–1765
[38] S2-UTN-RP-3001 "Inertial Sensor Ground Testing and Noise Model for LISA" ESTEC Contract 18233/04/NL/AG Final Technical Report (Nov 30, 2006)
[39] "Achieving geodetic motion for LISA test masses: ground testing results" L. Carbone, et al., Phys. Rev. Lett. 91, 151101 (2003)
[40] S2-ASD-RS-3005, Issue 5 Rev. 1 "IS Subsystem Requirement Specification" (June 15, 2007)
[41] "LISA Path finder: the experiment and the route to LISA" M Armano, et al., Class. Quantum Grav. (2009 To appear)
[42] "Upper limits to surface force disturbances on LISA proof masses and the possibility of observing galactic binaries" L. Carbone, et al. Physical Review D 75, 042001 (2007).
[43] "Temporal Extent of Surface Potentials between Closely Spaced Metals" S. E. Pollack et al., Phys Rev. Lett. 101, 071101 (2008)

[44] "Thermal gradient-induced forces on geodesic reference masses for LISA" L. Carbone, et al., Physical Review D 76, 102003 (2007)
[45] "Direct force measurements for testing the LISA Pathfinder gravitational reference sensor"A Cavalleri, et al.,. (2009 To appear)
[46] "A new torsion pendulum for testing the limits of free-fall for LISA test masses" A. Cavalleriet al., Class. Quantum Grav. (2009 To appear).
[47] S2-CGS-PL-3002 Issue, "Inertial sensor s/s and inertial sensor head assembly integration & verification plan" (March 2, 2007)
[48] J.K. Ziemer, *et al*, "Delivery of Colloid Micro-Newton Thrusters for the Space Technology 7 Mission", *Proceedings of the 44th AIAA Joint Propulsion Conference*, Hartford, CT, July 2008, AIAA 2008-4826.
[49] D. Nicolini, "LISA Pathfinder Field Emission Thruster System Development Program", Proceedings of the 30th International Electric Propulsion Conference, Florence, Italy, September 2007, IEPC 2007-363.
[50] C. Scharlemann, *et al*, "Development and Test of an Indium FEEP Micropropulsion Subsystem for LISA Pathfinder", *Proceedings of the 43rd AIAA Joint Propulsion Conference*, Cincinnati, OH, July 2007, AIAA 2007-5251.
[51] I. Rodriguez and G. Brown, "LISA Articulation Mechanism Update," LISA Project internal report (September 2005).
[52] Space Science Dept of Johns Hopkins Applied Physics Laboratory and Guidance and Control Department of Stanford University, "A satellite freed of all but gravitational forces: Triad," J. Spacecraft and Rockets **11**, 637 (1974).
[53] S. Buchman *et al.*, "The design and testing of the Gravity Probe B suspension and charge control systems," in Laser Interferometer Space Antenna, Second International LISA Symposium on the Detection and Observation of Gravitational Waves in Space, edited by W. M. Folkner (AIP, Woodbury, New York, 1998).
[54] T. T. Hyde *et al.*, "Pointing acquisition and performance for the laser interferometry space antenna mission," Class. Quant. Grav. **21**, S635 (2004).
[55] P. Maghami *et al.*, "Control of the Laser Interferometer Space Antenna," in Proceedings of the 18th International Symposium on Space Flight Mechanics, (2004).
[56] P. Gath, "DFACS Design for LISA," EADS Astrium GmbH internal report number LISA-ASD-TN-2002 (May 2006).
[57] P. G. Maghami *et al.*, "An acquisition control for the laser interferometer space antenna," Class. Quant. Grav. **22**, S421 (2005).
[58] P. G. Maghami *et al.*, "Acquisition Strategies for LISA," LISA Project internal report (February 2006).
[59] P. G. Maghami and T. Hyde, "Laser interferometer space antenna dynamics and controls model," Class. Quant. Grav. **20**, S273 (2003).
[60] H. Jörck, "End-to-End Simulation for LISA," EADS Astrium GmbH internal report number LISA-ASD-TN-2001 (September 2005).
[61] W. Fichter *et al.*, "LISA Pathfinder drag-free control and system implications," Class. Quant. Grav. **22**, S139 (2005).
[62] P. Gath *et al.*, "Drag Free and Attitude Control System Design for the LISA Pathfinder Mission," in AIAA Guidance, Navigation, and Control Conference and Exhibit, (2004). AIAA-2004-5430
[63] P. Maghami, "Space Technology 7, 18-DOF Mode Control Design Document," JPL Document No. D-34555 (March 2006).

[64] P. G. Maghami *et al.*, "Control of the ST7 Disturbance Reduction System Flight Experiment," in Proceedings of the 6th International LISA Symposium, edited by S. M. Merkowitz and J. Livas (American Institute of Physics Conference Proceedings, New York, 2006).

[65] "NASA Program and Project Management Processes and Requirements", NASA

5 List of Acronyms

Acronym	Definition
ACS	Attitude Control System
ADC	Analog-To-Digital Converter
ANU	Australian National University
AOM	Acousto-Optic Modulator
ARC	Austrian Research Centers
ASIC	Application Specific Integrated Circuit
CBE	Current Best Estimate
CCD	Charge Coupled Device
CDR	Critical Design Review
CFRP	Carbon Fiber Reinforced Plastic
CM	Caging Mechanism
CMA	Charge Management Assembly
CMNT	Colloid Micronewton Thruster
CTE	Coefficient Of Thermal Expansion
DAC	Digital-To-Analog Converter
DC	Direct Current
DCIU	Digital Control Interface Unit
DFC	Drag Free Control
DOF	Degrees Of Freedom
DPLL	Digital Phase-Locked Loop
DRS	Disturbance Reduction System
EBB	Elegant Breadboard
EDX	Energy Dispersive X-Ray
EH	Electrode Housing
EM	Engineering Model
EOM	Electro-Optic Phase Modulator
ESA	European Space Agency
FEE	Front End Electronics
FEEP	Field Emission Electric Propulsion
FLT2B	Formal Life-Test 2b
FPGA	Field Programmable Gate Array
GPS	Global Positioning System
GRACE	Gravity Recovery And Climate Experiment
GRS	Gravitational Reference Sensor
GSE	Ground Support Equipment
GSFC	NASA Goddard Space Flight Center
GW	Gravitational Wave
IDR	Instrument Delivery Review
IG	Interferometry Gate
IMS	Interferometry Measurement System
ISM	Interferometry Significant Milestones
ITAT	Integrated Technical Advisory Teams
JPL	Jet Propulsion Laboratory
LISA	Laser Interferometer Space Antenna
LLD	Launch Lock Devices
LMIS	Liquid Metal Ion Source
LO	Local Oscillator
LPF	LISA Pathfinder
LTP	LISA Test Package
MBW	Measurement Bandwidth
MDR	Mission Definition Review
MOFA	Master Oscillator Fiber Amplifier
MRD	Mission Requirements Document
MSE	Mission Systems Engineering
NCO	Numerically Controlled Oscillator
Nd:YAG	Neodymium-Doped Yttrium Aluminum Garnet
NEP	Noise Equivalent Power
NPRO	Non-Planar Ring Oscillator

Acronym	Definition
OA	Optical Assembly
OATM	Optical Assembly Tracking Mechanism
PAA	Point Ahead Actuator
PDR	Preliminary Design Review
PM	Proof Mass
PMS	Phase Measurement System
PSD	Power Spectral Density
PZT	Lead Zirconium Titanate Or Piezoelectric Transducer
QPD	Quadrant Photodiode
RF	Radio Frequency
RPSD	Root Power Spectral Density
RSS	Root Sum Squared
S/C	Spacecraft
ScRD	Science Requirements Document
SEM	Scanning Electron Microscope
SIM	Space Interferometry Mission
ST7	Space Technology 7
TDI	Time Delayed Interferometry
TRIP	Technology Readiness And Implementation Plan
TRL	Technology Readiness Level
TRP	Technology Readiness Programme
TRR	Test Readiness Review
UFLIS	University Of Florida LISA Interferometry Simulator
ULE	Ultra-Low Expansion Glass
UV	Ultraviolet
Yb:YAG	Ytterbium-Doped Yttrium Aluminum Garnet